JET EXPANSIONS: RESTRUCTURING LLM COMPUTATION FOR MODEL INSPECTION

Anonymous authors
Paper under double-blind review

ABSTRACT

Large language models are becoming general knowledge engines for diverse applications. However, their computations are deeply entangled after training, resisting modularization which complicates interpretability, auditing, and long-term maintenance. We introduce Jet Expansions, a framework for expanding computational graphs using jet operators that generalize truncated Taylor series. Our method systematically decomposes language models into explicit input-to-output computational paths and complementary remainders. This *functional decomposition* provides a principled, knife-like operator for cutting through entanglement in LLMs, enabling scalable model inspection. We demonstrate how Jet Expansions ground and subsume the popular interpretability technique Logit Lens, reveal a (super-)exponential path structure with respect to recursive residual depth, and support several interpretability applications, including sketching a transformer language model with -gram statistics extracted from its computations and indexing model toxicity levels without curated benchmarks.

1 INTRODUCTION

Symbolic AI systems stores knowledge in *modular, addressable units*: rules, facts, or graphs that mirrors human reasoning (Xu et al., 2025). Large language models (LLMs), by contrast, disperse knowledge across billions of entangled parameters. This mismatch between *computation layout* and *knowledge layout* is at the heart of the opacity of LLMs, creating practical challenges. Once trained, LLMs cannot be easily audited, updated, or corrected: removing toxic knowledge, deleting private information, or incorporating new policies is far from straightforward (Kadhe et al., 2024; Li et al., 2025). In contrast, such operations could be trivial in systems that structure knowledge into addressable units, such as symbolic systems. The opacity of LLM computations thus raises concerns about transparency, accountability, and long-term maintenance in high-stakes domains such as healthcare (Smith, 2021; Liu et al., 2023; Comeau et al., 2025) and robotics (Wachter et al., 2017; Raptis et al., 2024; Fernández-Becerra et al., 2024).

Existing interpretability methods often take a *data-then-explanation* approach: curate inputs, hypothesize which sub-computations matter, and observe activations to refine the hypothesis (Wang et al., 2022; Meng et al., 2022; Goldowsky-Dill et al., 2023). But the real challenge is structural: LLM computations are *entangled*, preventing us from isolating embedded knowledge into meaningful units. While one can gain valuable insights with data-driven interpretability approaches, we posit that the ability to reorganize computation into smaller, less entangled, end-to-end components "mechanically" – rather than "experimentally" – is central to tackle such issue at scale.

We present *Jet Expansions*, a principled, general-purpose framework for manipulating LLM computations. Noting that LLMs are particular types of residual networks (He et al., 2016; Vaswani et al., 2017), our key idea is to recursively expand residual computations using *jet operators* (Ehresmann, 1951), the functional counterpart of truncated Taylor series. This process yields functional rewritings of the model into two parts: (i) explicit input→output polynomial functions, which we call *jet paths*, and (ii) complementary nonlinear remainders. Crucially, Jet Expansions operates at a functional level, requiring no additional data, nor training. We show that jet expansions encompass existing interpretability tools such as the logit lens (nostalgebraist, 2021b), and extend them to new instantiations such as jet n-grams. This enables data-free, symbolic sketches of transformer LLMs and allow us to perform global interpretability studies. Figure 1 illustrates the pipeline.

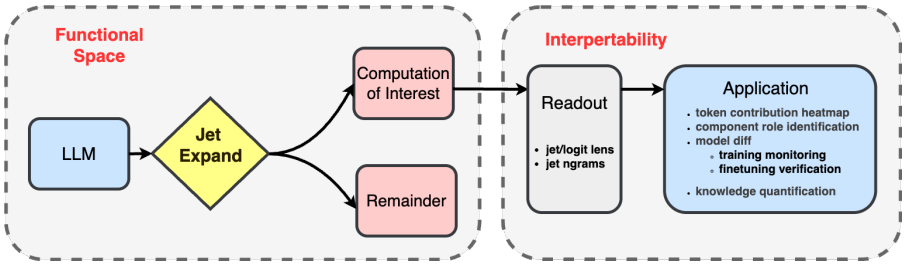

Figure 1: Jet Expansions restructure residual computations into explicit input→output paths and a complementary remainder. From these paths we can extract logits, and n-grams without retraining or additional data. These readouts support downstream applications such as token contribution heatmaps, model comparison, training monitoring, and fine-tuning verification.

We validate our framework through case studies across diverse autoregressive LLMs (*GPT*, *Llama*, *OLMo*). Jet expansions enable several empirical usages: i) understanding inner mechanisms (Section 5.2.1); ii) assessing fine-tuning effects, e.g. quantifying toxicity levels with jet n-grams, showing RLHF alignment (Bai et al., 2022) reduces but does not eliminate toxic knowledge (Section 5.2.2); iii) analyzing pretraining dynamics, e.g. tracking how bi-grams such as "at least" are promoted then suppressed in *OLMo* (Appendix F). These results demonstrate that jet expansions provide a powerful, data-free operator for restructuring LLM computations, paving the way for more transparent, interpretable, and maintainable foundation models.

Our contributions.

1. A new angle on interpretability: treating it as *function decomposition*, rather than input-driven attribution or circuit identification on particular datasets.
2. A principled theoretical framework, based on jet operators, formally grounding existing tools such as *logit lens* (nostalgebraist, 2021b;a) and *path expansion* (Elhage et al., 2021).
3. Preliminary but wide-ranging case studies, revealing insights into LLM internal mechanisms, training dynamics, and toxicity levels.

2 Background and Preliminaries

Language models as residual networks. We focus on transformer language models (Vaswani et al., 2017), which are residual networks (He et al., 2016) consisting of L stacked residual blocks sandwiched between an encoder Enc and a decoder Dec. Formally, the full computation is

$$f = \mathrm{Dec} \circ \left(\bigcirc_{\ell=1}^{L} (\mathrm{id} + \gamma_\ell)\right) \circ \mathrm{Enc}, \tag{1}$$

where γ_ℓ is the non-linear transformation in block ℓ. Unrolling the recursion, the hidden state after ℓ blocks is

$$h_\ell = h_0 + \textstyle\sum_{j=1}^{\ell} \gamma_j \circ h_{j-1}, \qquad h_0 = \mathrm{Enc}(z). \tag{2}$$

This recursive form makes clear that residual links accumulate contributions from all preceding layers. We adopt the notion of *residual streams* (Elhage et al., 2021), where the computation can be viewed as nested terms entangling contributions across blocks (see also (Veit et al., 2016)). Table 1 summarizes the notation.

Taylor expansions and jets. To handle nonlinearities when restructuring residual computations, we rely on *jets* (Ehresmann, 1951), which generalize Taylor expansions. For $f \in C^{k+1}(\mathbb{R}^d, \mathbb{R}^d)$, Taylor's theorem at base point x_0 gives

$$f(x) = f(x_0) + \textstyle\sum_{j=1}^{k} \frac{1}{j!}\, \mathrm{D}^j f(x_0)\,(x - x_0)^{\otimes j} + O(\|x - x_0\|^{k+1}). \tag{3}$$

The k-th order *jet operator* abstracts this expansion as

$$\mathrm{J}^k f \colon \mathbb{R}^d \to P^k, \qquad \mathrm{J}^k f(x_0)(x) = f(x_0) + \textstyle\sum_{j=1}^{k} \frac{1}{j!}\, \mathrm{D}^j f(x_0)\,(x - x_0)^{\otimes j}, \tag{4}$$

or equivalently, by leaving the polynomial action implicit,

$$\mathrm{J}^k f(x_0) = f(x_0) + \sum_{j=1}^{k} \tfrac{1}{j!}\, \mathrm{D}^j f(x_0).$$

Intuitively, $\mathrm{J}^k f(x_0)$ captures the local structure of f up to order k, and we write $f(x) \approx_k \mathrm{J}^k f(x_0)(x)$ to indicate agreement up to order k. Jets thus provide a principled operator for rewriting residual computations into decomposable pieces.

Remark 1 (Base points and variables as functions). When tracing back to the input $z \in \mathcal{X}$, base points x_0 and variables x may themselves depend on z. In that case, jets define maps $\mathcal{X} \to \mathcal{Y}$ via $\mathrm{J}^k f(x_0(z))(x(z))$. For brevity, we often omit explicit dependence on x when clear from context. (See Appendix A for details.)

Table 1: Summary of notation used in the paper.

Symbol	Meaning	Symbol	Meaning
$\mathcal{X}$	Input space	L	Depth (no. of blocks)
V	Vocabulary size	id	Identity map
$\mathcal{Y} = \mathbb{R}^V$	Output logits	U	Unembedding matrix
d	Hidden dimension	ν	Final normalization
$f : \mathcal{X} \to \mathcal{Y}$	Full network	h_ℓ	Hidden state at layer ℓ
$\mathrm{Enc} : \mathcal{X} \to \mathbb{R}^d$	Encoder	β_ℓ	Residual block at layer ℓ
$\mathrm{Dec} : \mathbb{R}^d \to \mathcal{Y}$	Decoder	γ_ℓ	Residual transform inside block ℓ
x_0	Base point (center)	x	Variable
$D^j f(x_0)$	j-th differential	$(x - x_0)^{\otimes j}$	j-fold tensor product
$\mathrm{J}^k f(x_0)$	k-jet at x_0	$\mathrm{J}^k f$	Jet operator
P^k	Degree-k polynomial space		

3 Related Work

Mechanistic interpretability and path rewriting. A large body of work has sought to interpret the inner computations of large language models. One prominent category is *mechanistic interpretability* (MI) (Ferrando et al., 2024), which aims to reverse-engineer model computations by identifying, clustering, and labeling behaviors (Shah et al., 2024; Meng et al., 2022; Bricken et al., 2023) and attributing them to specific components, such as MLPs (Geva et al., 2021; 2022) or circuits (Conmy et al., 2023; Ferrando & Voita, 2024). However, these approaches often restrict analysis to atomic components (neurons, layers, or weights), which may not reveal the *full* mechanism of information processing. For example, Templeton et al. (2024) highlight the difficulty of drawing conclusions at the neuron level compared with higher-level feature representations, while Bolukbasi et al. (2021); Goldowsky-Dill et al. (2023) emphasize that many findings depend heavily on the chosen data distribution. A second category of approaches attempts explicit *path rewriting*. Veit et al. (2016) expand residual networks into paths of varying length to study gradient behavior. Elhage et al. (2021) decompose one- and two-layer transformers into sums of unigram and bigram computation paths. Goldowsky-Dill et al. (2023) extend this line of work by developing path patching methods that aim to preserve functional faithfulness while isolating specific behaviors. Aligning with the second category, our approach manipulates functions directly rather than activations. It requires neither probe datasets (Belrose et al., 2023) nor sampling (Conmy et al., 2023; Ferrando & Voita, 2024; Voita et al., 2024). By allowing arbitrary portions of computation to be isolated from the monolithic transformer, jet expansions abstract and generalize prior path-based characterizations (Veit et al., 2016; Elhage et al., 2021), including nonlinear components often ignored or simplified (e.g. layer norms and MLPs).

N-gram models as symbolic counterparts. n-gram models, dating back to Shannon (1948), represent one of the earliest symbolic approaches to language modeling. They store explicit probabilities of token sequences, e.g. $\Pr(w_i \mid w_{i-1}, \ldots, w_{i-n+1})$, in tabular form. This makes their *knowledge layout identical to their computation layout*: each sequence has a directly addressable probability entry. Such symbolic modularity enabled early successes in language modeling (Goodman, 2001) and tasks like machine translation (Brants et al., 2007). While later work combined n-grams with networks (e.g. Liu et al., 2024), recent studies revisit their role in relation to LLMs: for instance, analyzing the ability of transformers to simulate n-gram statistics (Svete & Cotterell, 2024) or measuring agreement between LLM predictions and n-gram rulesets (Nguyen, 2024).

Taylor expansions and jets. Taylor expansions are popular tools in analyzing learning behaviours (Jastrzebski et al., 2017), notably with linearization ($k = 1$). For example, Belrose et al. (2024) applied Taylor expansion on the loss function to demonstrate the learning preference of neural network models. Xu et al. (2022) used a second-order Taylor expansion over the data distribution to interpret optimal features. The generalized jet notions was introduced in machine learning in the context of automatic differentiation tools by Bettencourt et al. (2019), and is an experimental feature in Jax (Bradbury et al., 2018), but has been studied before (see e.g. Griewank & Walther, 2008). We leverage jets not merely as approximation tools, but as operators to restructure residual computations in LLMs into explicit input→output paths and complementary remainders.

4 Restructuring LLM Computation with Jet Expansions

Traditional interpretability tools (e.g., probing, distillation, attention visualization) provide only partial and often data-dependent insights; they do not entirely reorganize the underlying computation. Jets approximate functions locally and, crucially, can be leveraged as a *carving operator* that makes otherwise entangled computations decomposable.

4.1 Linear case: easy to restructure

We begin with the linear case, where residual computations can be reorganized ***exactly*** without any approximation. Consider a linear residual network, with $\gamma_\ell(x) = A_\ell x$ for some $A_\ell \in \mathbb{R}^{d\times d}$, encoder $\mathrm{Enc} = E$, and $\nu = \mathrm{id}$. Then

$$f = \mathrm{Dec} \circ \Big(\bigcirc_{\ell=1}^{L} (\mathrm{id} + \gamma_\ell) \Big) \circ \mathrm{Enc} = U\Big(\sum_{S\subseteq 2^{[L]}} \prod_{l\in S} A_l \Big) E = \sum_{S\subseteq 2^{[L]}} f_S, \tag{5}$$

where $2^{[L]}$ is the power set of $[L] = \{1, \ldots, L\}$ and each path $f_S = U\Big(\prod_{l\in S} A_l\Big)E = UW_S E, W_\emptyset = I$, is itself a linear map from $\mathcal{X}$ to $\mathcal{Y}$. Thus, the entire network can be written as the sum of 2^L explicit input-to-output paths f_S. This exact decomposition makes linear residual networks intrinsically easy to restructure. In the nonlinear case, however, such a clean decomposition no longer holds, motivating the use of jets.

4.2 Nonlinear case: jets to the rescue

$\mathrm{J}^k f(x_0)$ encodes all information about a function f up to order-k derivatives at a base point x_0, providing a vector-free representation of its local behavior. This makes jets a principled tool for reorganizing computations in LLMs. Lemma 1, proved in Appendix A, formalizes their *disentangling property*: the jet at a sum of inputs can be written as a convex combination of jets at the individual inputs, up to higher-order error. This allows us to carve apart nested residual terms into separate, analyzable contributions (Figure 2).

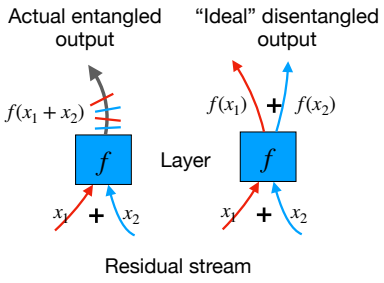

Figure 2: Convex combinations of jets disentangle a residual stream h_ℓ (a sum of terms) into sub-streams in function space.

Lemma 1 (Disentanglement of Jets)**.** *Let $f \in C^\infty(\mathbb{R}^d, \mathbb{R}^d)$, $k \in \mathbb{N}$, $N \in \mathbb{N}^+$, $\{x\}_{i=1}^N$ be a set of* jet base points*, and $w \in \triangle^{N-1} \subset \mathbb{R}^N$ be a set of* jet weights *(i.e., $w_i \geq 0$, $\sum_i w_i = 1$). Define the sum $\bar{x} = \sum_{i=1}^N x_i$ and $r = \max_i w_i \|x_i - \bar{x}\|$. Then the k-jet of f at the sum $\bar{x}$ satisfies*

$$\mathrm{J}^k f\left(\sum_{i=1}^N x_i\right) = \sum_{i=1}^N w_i \, \mathrm{J}^k f(x_i) \; + \; O(r^{k+1}).$$

Example 1 (Jet expansion of ReLU). Consider the ReLU activation function $\gamma : \mathbb{R} \to \mathbb{R}^+$ defined as $\gamma(x) = [x]_+$. For $x > 0$, $\gamma'(x) = 1$. For $x < 0$, $\gamma'(x) = 0$. Higher order derivatives are zero almost every. If $x = x_1 + x_2$, then for almost every x, there exist $w \in \triangle^1$ such that

$$\gamma(x_1+x_2) = w_1 \mathrm{J}^1\gamma(x_1)(x_2) + w_2 \mathrm{J}^1\gamma(x_2)(x_1) = w_1(\gamma(x_1)+\gamma'(x_1)x_2) + w_2(\gamma(x_2)+\gamma'(x_2)x_1).$$

In other words, for almost every center $x = x_1 + x_2$ there exists a convex combinations of jets that is exact. Indeed, if either $x_1, x_2 > 0$ or $x_1, x_2 < 0$, then any convex combination is exact. If only

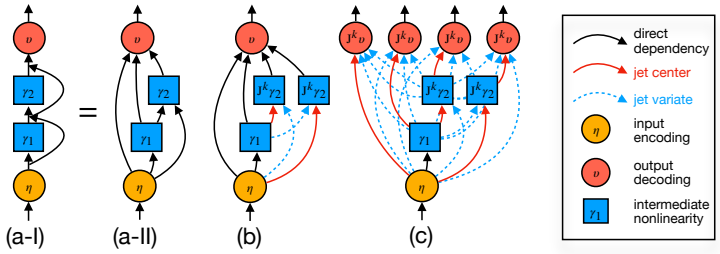

Figure 3: Carving a two-block network. (a) Nested entanglements. (b) Inner expansion at γ_2. (c) Outer expansion at Dec, yielding 4 explicit paths.

one of the two terms is positive, say $x_1 > 0$ and $x_2 < 0$, then we can set $w_1 = 1$ if $x_1 + x_2 \geq 0$ and $w_1 = 0$ otherwise ($w_2 = 1 - w_1$). The specular argument applies for the case $x_1 < 0$ and $x_2 > 0$. From a global perspective, we can think of jet weights $w_i = w_i(x_1, x_2)$ as functions of x_1 and x_2, rather then constants – and in the ReLU case, we obtain (almost everywhere) an exact first-order expansion. Conversely, one can see that the 0-th order jet expansion of γ is not globally exact.

4.2.1 Motivating example: carving a two-block residual network.

Now we consider how to use jets to carve a typical computation graph. We begin with the simplest nontrivial case: a network with two residual blocks. Using Equation (1), its full computation is

$$f = \mathrm{Dec} \circ \Big(\underbrace{\mathrm{Enc}}_{x_0} + \underbrace{\gamma_1 \circ \mathrm{Enc}}_{x_1} + \underbrace{\gamma_2 \circ \big(\mathrm{Enc} + \gamma_1 \circ \mathrm{Enc}\big)}_{x_2} \Big).$$

The nested parentheses entangle contributions: the outer (purple) grouping mixes everything, while the inner (orange) ties γ_2 to both x_0 and x_1. Traditional MI would select paths syntactically, ignoring this nesting. Jets let us cut both levels systematically.

Step 1: Inner expansion. At γ_2, taking $\{x_0, x_1\}$ as jet base points and using Lemma 1, the residual stream $x_2 = \gamma_2 \circ (x_0 + x_1)$ can be decomposed as

$$x_2 \;\approx_k\; J^k\gamma_2(x_0 + x_1) = \underbrace{w_0 J^k\gamma_2(x_0)}_{x_{20}} + \underbrace{w_1 J^k\gamma_2(x_1)}_{x_{21}} + O(r^{k+1}),$$

so the original entangled stream x_2 separates into two sub-streams, as illustrated in Figure 3(b).

Step 2: Outer expansion. At Dec, the jet base points are updated from $\{x_0, x_1, x_2\}$ to $\{x_0, x_1, x_{20}, x_{21}\}$ after previous expansion. Using Lemma 1 and jet algebra (Proposition 1), yields

$$\begin{aligned} f \;\approx_k\; J^k\mathrm{Dec}(x_0 + x_1 + x_{20} + x_{21}) &= \underbrace{\bar{w}_0 J^k(\mathrm{Dec}\circ\mathrm{Enc})}_{f_\emptyset} + \underbrace{\bar{w}_1 J^k(\mathrm{Dec}\circ\gamma_1\circ\mathrm{Enc})}_{f_{\{1\}}} \\ &+ \underbrace{\bar{w}_2 J^k(\mathrm{Dec}\circ(w_0 J^k(\gamma_2\circ\mathrm{Enc})))}_{f_{\{2\}}} + \underbrace{\bar{w}_3 J^k(\mathrm{Dec}\circ(w_1 J^k\gamma_2(\gamma_1\circ\mathrm{Enc})))}_{f_{\{1,2\}}} + O(r^{k+1}). \end{aligned}$$

corresponding to four distinct input→output paths $f_\emptyset, f_{\{1\}}, f_{\{2\}}, f_{\{1,2\}}$. This is shown in Figure 3(c). Each term aligns with what one might pick manually as a "path" in the network, but here it arises *systematically* from the jet expansion. This toy example illustrates the two key principles of our approach: recursive jet expansion of residual computations, and the use of convex combinations (Lemma 1) to isolate entangled contributions. In deeper networks with many blocks, however, manual expansion becomes infeasible. This motivates our general-purpose algorithmic framework.

4.3 General framework

We now develop `jet_expand`, the general algorithm for expanding residual computations into atomic input-output paths. Algorithm 1 describes the core operation. At each block l (or at the final decoding nonlinearity), the algorithm applies Lemma 1 to a set of jet base points $\mathcal{C}$. The output is (i) a set of expanded polynomial terms ξ, (ii) a nonlinear remainder which collects both the higher-order Taylor terms from Equation (3) and the approximation error from Lemma 1. A key property is that *jet base points can themselves be outputs of earlier expansions*. This enables recursive application of `jet_expand` throughout the network, effectively "unrolling" the computation graph into explicit input→output paths. At the final layer, this gives a functional rewriting of the model: if $(\xi_L, \delta_L) = \texttt{jet\_expand}(f, L, \mathcal{C}, k)$ for some choice of centers $\mathcal{C}$ and order k, then

Algorithm 1 `jet_expand`$(f, l, \mathcal{C}, k)$

Require: Residual net f, block index $l \in [L]$; jet base points $\mathcal{C} = \{x_i\}_{i=1}^N$; jet order $k \in \mathbb{N}$.
Ensure: Expanded jet terms ξ with weights w, and remainder δ.

$\xi \leftarrow \{\, w_i \mathrm{J}^k \gamma_{l+1}(x_i) \,\}_{i=1}^N$
if $l < L$ **then**
  $\xi \leftarrow \xi \cup \{\, w_i \mathrm{J}^k \mathrm{id}(x_i) \,\}_{i=1}^N$
  $\delta \leftarrow h_{l+1} - \sum_{e \in \xi} e$
else
  $\delta \leftarrow \mathrm{Dec} \circ h_L - \sum_{e \in \xi} e$

$$f(z) \;=\; \textstyle\sum_{e \in \xi_L} U\, e(z, w) \;+\; \delta_L(z, w), \qquad \text{for } w \in \triangle^{N-1}. \tag{6}$$

So, the model can be rewritten as a sum of expanded terms (explicit paths) plus a remainder.

Remark 2 (Remainders and weights). Remainders δ need not vanish, so jet expansions should be read as *rewritings* rather than strict approximations. Special cases (linear or ReLU-only networks) admit exact expansions. Weights w can be fixed (e.g. uniform) or optimized to minimize δ (we used gradient descent in Sec. 5.2.1). Empirically, remainders are often small and expansion logits nearly collinear with model outputs.

Lemma 2. *Residual networks with only ReLU nonlinearites admit exact first-order jet expansions.*

Runtime. The runtime of algorithm 1 is negligible, as it operates directly on the original computational graph. Evaluating ξ and δ at $z \in \mathcal{X}$ requires computing kth-order jets at cost $O(|\mathcal{C}|(F + kB))$, where F and B denote forward and backward passes of q. In practice, higher-order jets can be computed efficiently via recurrence relations and standard automatic differentiation primitives such as Jacobian-vector products (JVPs) (Griewank & Walther, 2008; Bettencourt et al., 2019). Appendix B reports empirical runtime scaling of our implementation with jet order k.

5 Applications of Jet Expansions

5.1 Theoretical applications

The principled framework of jet expansions allows us to ***ground*** existing techniques in a unified theoretical framework and derive new ones. Here we introduce several expansions as direct applications of the `jet_expand` algorithm, which set the stage for the empirical case studies.

(Super-)exponential expansion. Alg. 2 extends our two-block example to arbitrary depth, producing 2^L paths via uniform jet weights. This mirrors Veit et al. (2016)'s exponential view of residual networks, but in an explicit and principled way. For $k \geq 1$, each polynomial term can be decomposed further by degree, isolating higher-order block interactions, hinting at a *super-exponential* ensemble perspective which we leave as future work.

Algorithm 2 `exp_jet_expansion`(f, k)

Require: Residual computation f; order $k \in \mathbb{N}$.
Ensure: Expanded paths ξ with uniform weights ($|\xi| = 2^L$) and remainder δ.

$\xi \leftarrow \{\mathrm{Enc}, \gamma_1 \circ \mathrm{Enc}\}$
for $l \in [L]$ **do**
  $(\xi, \delta) \leftarrow \texttt{jet\_expand}(f, l, \xi, k)$
  $\xi \leftarrow \{e(\cdot, 1/|\xi|) \mid e \in \xi\}$ ▷ uniform weighting

Jet lenses and the logit lens. The *logit lens* (nostalgebraist, 2021b; Geva et al., 2021; 2022; Merullo et al., 2023; Belrose et al., 2023) is a popular interpretability tool, applying the decoder to intermediate hidden states as follows:

$$\mathrm{LogitLens}_l(z) = \mathrm{Dec}(h_l(z)) = U\nu(h_l(z)) = J^0 \mathrm{Dec}\big(h_l(z)\big)(h_L(z)).$$

Indeed, $\mathrm{Dec}(x) \approx_{k=0} J^0\mathrm{Dec}(h_l(z))(x) = \mathrm{Dec}(h_l(z))$. Thus the logit lens is simply the zeroth-order expansion at final layer with h_l as the jet base point $\texttt{jet\_expand}(f, L, \{h_l\}, 0)$. This suggests two generalizations, which we dub *iterative* and *joint* jet lenses, respectively. The ***iterative jet lens*** is a direct extension of the logit lenses with higher order jets: $\texttt{jet\_expand}(f, L, \{h_l\}, k)$. The ***joint jet lenses*** are expansions obtained through $\texttt{jet\_expand}(f, L, \{\gamma_l \circ h_{l-1}\}_{l\in[L]}, k)$ that are aimed at highlighting the residual contributions of each block nonlinearity, rather than the iterative refinement of the residual stream.

Jet bi-grams and skip-n-gram statistics. Our framework allows us to extract n-gram statistics *directly from the language model*, without any probing data. Specifically, we systematically evaluate selected jet paths (the expanded polynomial terms) over the entire input space, usually the vocabulary and its Cartesian products, to obtain symbolic n-gram tables. For example, bi-grams statistics related to $\mathbb{P}_f(z_n|z_{n-1}, \dots)$ can be computed by evaluating bi-gram paths, which we can obtain by expanding the LLM with Algorithm 2 and filtering out all paths that involve self-attention modules. Specifically in our case studies (Section 5.2), we focus on encoding-decoding bi-gram path, obtainable via expanding the LLM with $\texttt{jet\_expand}(f, L, \{\mathrm{Enc}\}, k = 0)$, and the bi-gram paths involving up to one MLP module, which can also be obtained via applying Algorithm 1 twice. We can obtain skip-n-gram statistics relating to $\mathbb{P}_f(z_n|z_{n-1}, \dots, z_{n-2}, \dots, z_1, \dots)$, where dots indicate any number of interceding tokens, by evaluating jet paths with self-attentions (the fewer self-attentions, the lower the n) and isolated single query-key products. And uni-grams can be obtained via finding the stable state of the Markov transition equation defined via the conditional bi-grams.

These Jet n-gram statistics generalize Elhage et al. (2021) to provide a *data-free* sketch of an LLM, casting it into a symbolic n-gram database. They also enable symbolic model comparison ("diffing") between any two models with a shared vocabulary, in contrast to parameter-space differencing, which is architecture-dependent and harder to interpret. Details are given in Appendix C.

5.2 Empirical Case Studies

We illustrate two interpretability applications of jet expansions: analyzing the *inner workings* of LLMs and assessing the *effects of fine-tuning*. Additional case studies are provided in Appendix F.

Setup. We experiment on open-source LLMs including *GPT-2* (Radford et al., 2019), *GPT-Neo* Black et al. (2021), *Llama* (Touvron et al., 2023a;b; Rozière et al., 2024), and *OLMo* (Groeneveld et al., 2024). N-gram experiments were run on 128-CPU servers with 1TB memory, while jet lenses were computed on a single laptop CPU. Jet weights were optimized by gradient descent; for n-grams we restrict to zeroth-order jets from embedding→MLP→unembedding. Algorithmic details and evaluation metrics are given in App. C and D.

5.2.1 Analyzing LLM inner working

Jet lenses. We use ***jet lenses*** to analyze LLMs' mechanism when processing individual examples. Figure 4 (top) visualize a joint jet lens for GPT-Neo 2.7B (Black et al., 2021) (other examples can be found in Appendix I). Here, a block contains one self-attention and one MLP module. All table cells depict top-1 tokens for the corresponding path, following conventions from prior work (Belrose et al., 2023). We observe that the joint jet lens captures the synergy among different blocks, as the model prediction is decomposed into several jet paths, as indicated by the percentages.

In this sense, the jet lenses with $k > 0$ may serve as tools to systematically discover such synergic behaviors. We also find that higher-orders ($k > 0$) help iterative lenses deliver more meaningful interpretations than the logit lens ($k = 0$) for *GPT-Neo-2.7B* (see Figures 8 to 10). This is potentially due to their capability to trace indirect impacts of early layers on the final logits, which were otherwise missing under logit lens. Our findings are consistent with nostalgebraist (2021a); Cancedda (2024) where naive implementations of logit lens are shown to fail on *GPT-Neo* model family. Figure 4 (bottom) present mean cosine similarities of joint and iterative jet lenses for various *GPT* models and orders, averaged over 100 example sentences. The similarities are high and close to 1 for various k, showing however different behavior across model families and sizes. This indicates jet expansions highly correlate with model outputs, potentially providing faithful interpretations. In particular, the right plot compares the similarities of the logits obtained through iterative jet lenses

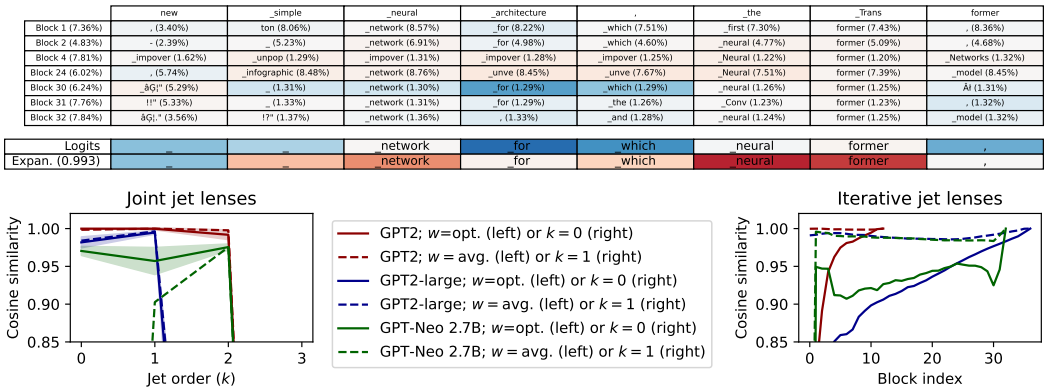

Figure 4: (**Top**) example of a joint jet lens on *GPT-Neo* 2.7*B* with $k = 1$, visualizing the seven blocks with highest average jet weights after optimization. Each table cell indicates the most likely token of the jet path related to each block nonlinearity. Optimized jet weight are in the brackets next to the most likely token. We used a diverging blue-to-red color map tracking logit scores, centered around zero. The second table with two rows shows the model logits (Logits) and the expansion logits (Expan.), with cosine similarity in brackets; in this case, all top-1 tokens perfectly coincide. (**Bottom**) plots of average cosine similarities between original and jet logits of joint (**left**) and iterative (**right**) lenses.

Table 2: MLPs in *OLMo*-7*B* and *Llama*-2-7*B* performing certain linguistic functions based on jet bi-grams extracted from the corresponding jet paths.

	OLMo-7*B*					*Llama*-2-7*B*			
MLP Index	1	3	9	17	19	6	7	18	19
Role	`-ly, -_else`	`-ing`	`-'t`	`-_than`	`-s`	`-ing`	`-es`	`-ing,-ity`	`-ly`
Δ logit after intervention	$-4.19, -3.35$	-0.58	-9.73	-4.26	-7.42	-14.61	-3.55	$-9.69, -11.93$	-9.14

for $k = 0$ (solid, line, the same as LogitLens) and for $k = 1$ (dashed lines), indicating an higher correlation of the latter with model outputs, potentially providing more faithful interpretations.

Jet paths of individual components. By examining the representative jet bi-grams that are captured by each MLP path, we find some MLPs perform special linguistic functions. For example, in *OLMo*-7*B*, the jet path which passes through the 3rd MLP promotes the addition of the "`-ing`" suffixes to the current token. Similar MLPs with certain linguistic functions are listed in Table 2. Note that the relationship between functions and components are not necessarily one-to-one mappings. Particularly we find that paths through multiple MLPs might work together to complete one linguistic function e.g. MLP 6 and MLP 18 in *Llama*-2-7*B* can add "`-ing`" suffix. This echos work on circuit discovery (Elhage et al., 2022; Conmy et al., 2023; Ferrando & Voita, 2024), where the role of each component cannot be easily dissected and multiple components collaborate.

5.2.2 Analyzing fine-tuning effect

Jet n-gram diffing provides a human-readable way to track knowledge shifts during fine-tuning.

Code fine-tuning. Comparing *Llama-2-7B* with its *Codellama* variants, jet bi-grams diffing highlights code-specific patterns such as "`**kwarg`" or "`Assertion`" (Table 3), confirming the acquisition of programming knowledge. This suggests jet bi-gram can be a tool for verifying if fine-tuning is effective in acquiring relevant knowledge.

RLHF alignment. While *ToxiGen* scores suggest detoxification of Llama-2-7B-Chat, jet bi-gram masses remain nearly unchanged (Table 4), indicating toxic associations persist in latent form. Challenging prompts from RealToxicityPrompts (Gehman et al., 2020) confirm that these associations can still be triggered. Thus, RLHF appears to mask rather than erase toxic knowledge, a finding revealed directly by data-free jet bi-gram indices. This showcases a potential application of jet bi-grams in constructing *data-free* indices that reveal embedded knowledge, offering complimentary views beyond traditional data-driven benchmark evaluations.

Table 3: The bi-grams before and after coding-finetuning. For space reason, we only show the bi-grams at every 50 ranks among the top 1000 bi-grams. We highlight the bi-grams that are relevant to coding, such as "**kwargs" a keyword in python programming. This demonstrate that our method has the capability to extract representative bi-grams that reflect fine-tuning quality.

Rank	LLAMA2-7B	CodeLLAMA-7B	CodeLLAMA-Python-7B
0	(_more, _than)	(_like, wise)	(_like, wise)
50	(_Now, here)	(_just, ification)	(_Like, wise)
100	(_system, atically)	(_in, _case)	(_all, udes)
150	(_all, erg)	(_get, ters)	(_no, isy)
200	(_on, ions)	(któber, s)	(output, ted)
300	(_other, world)	(_all, ud)	(Object, ive)
350	(_Just, ified)	(gebiet, s)	(_as, cii)
400	(_trust, ees)	(_Protest, s)	(_can, nab)
450	(_at, he)	(_deploy, ment)	(_transport, ation)
500	(_book, mark)	(Class, room)	(Tag, ging)
550	(_from,)	(_access, ory)	(_personal, ized)
600	(_WHEN, ever)	(_In, variant)	(_excess, ive)
650	(_where, about)	(_I, _am)	(_Add, itional)
700	(ag, ged)	(add, itionally)	(_**, kwargs)
750	(_he, he)	(_invalid, ate)	(name, plates)
800	(_all, anto)	(div, ision)	(_select, ive)
850	(_Tom, orrow)	(_process, ors)	(_Assert, ions)
900	(_for, ays)	(_Program, me)	(blog, ger)
950	(_Bach, elor)	(_set, up)	(_can, cellation)

Table 4: Toxicity indexes for *Llama*-2-7*B* and *Llama*-2-7*B-chat* using different methods: *ToxiGen*, jet bi-grams, and *RealToxicityPrompts* challenge prompting. Higher numbers indicate higher toxicity scores on the corresponding benchmarks and higher toxic knowledge possession for jet bi-grams.

	ToxiGen Score	Jet Bi-grams	RTP Challenging Prompts			
	Hartvigsen et al. (2022)	Mass of "toxic" bi-grams	No	Very mild	Medium	Hard
Llama-2-7*B*	21.25	0.03445	38%	49%	64%	88%
Llama-2-7*B-chat*	0.0	0.03377	23%	35%	64%	84%

6 Conclusion

We introduced *jet expansion*, a principled framework for restructuring the computational graphs of large language models. Specialized here to LLMs, our method systematically disentangles contributions of user-selected input→output paths from the overall computation, yielding interpretable functional components plus a complementary remainder. Operating directly in function space, jet expansions cut through entanglement (a "scalpel" for residual computation), respect residual structure (recursive expansion of skip connections), and are grounded in approximation theory (jets as generalized truncated Taylor operators). This enables modular inspection: one can pull out paths of interest (e.g., logit lens, n-gram paths) while bracketing the rest as remainder.

Limitations. Jet expansions are not strict function approximations in the Taylor sense; they *rewrite* the computation into interpretable polynomial terms plus a remainder. Remainder size and alignment with model outputs depend on the jet order k and weight choices (hyperparameters), and expansions are not unique (higher orders contain lower orders). While graph manipulation is lightweight, systematic evaluation of many (and higher-order) paths can be costly; heuristics or subsampling may be needed for large input spaces. Our n-gram studies focused on bi- and tri-grams; longer-context expansions are left to future work.

Implications and future work. We envision a Fourier-transform style decomposition for LLMs and jet expansions is perhaps only one way of choosing the basis. Theoretically, we aim to connect with attribution (e.g., Shapley values), and formalize model equivalence via jet spaces to ground model diffing. We see fruitful links to linear algebraic decompositions and to Markov/HMM viewpoints (e.g., structured decoding (Zhang et al., 2023)). We will also study the implications of the super-exponential path growth with depth. Practically, beyond longer n-grams, we will develop safety/transparency tools (e.g., search features for unwanted associations or PII leakage). Finally, although our experiments are mainly observational, `jet_expand` may help guide *interventions*, complementing causal tracing and path patching.

Ethics Statement

This work focuses on developing a mathematical framework (jet expansions) for analyzing large language models. Our study does not involve human subjects, proprietary or sensitive data, or experiments that raise privacy, security, or legal concerns. We acknowledge that interpretability tools may potentially be misused to extract or expose harmful content (e.g., toxic or private knowledge) embedded in pretrained models. We use the public datasets for LLM toxicity research. We emphasize that our intent is to promote transparency, safety, and responsible analysis of LLMs, and we recommend future work carefully consider these implications in line with the ICLR Code of Ethics.

Reproducibility Statement

We have taken steps to ensure the reproducibility of our results. All definitions, assumptions, and theoretical proofs are included in the main text and appendix. Detailed algorithms (Algorithm 1, Algorithm 2) and mathematical derivations are provided for clarity. Experimental procedures, model families used (GPT-2, GPT-Neo, LLaMA, OLMo), and metrics are described in Section 5.2 and Appendix D. We will open-source the code implementing jet expansions, extracting jet n-grams, and reproducing jet lenses, ensuring that all empirical results reported can be replicated.

LLM Usage Acknowledgments

We used LLMs to assist with grammar and writing polishing. All equations, analysis, and research contributions are entirely our own.

References

Yuntao Bai, Andy Jones, Kamal Ndousse, Amanda Askell, Anna Chen, Nova DasSarma, Dawn Drain, Stanislav Fort, Deep Ganguli, Tom Henighan, et al. Training a helpful and harmless assistant with reinforcement learning from human feedback. *arXiv preprint arXiv:2204.05862*, 2022.

Nora Belrose, Zach Furman, Logan Smith, Danny Halawi, Igor Ostrovsky, Lev McKinney, Stella Biderman, and Jacob Steinhardt. Eliciting latent predictions from transformers with the tuned lens. *arXiv preprint arXiv:2303.08112*, 2023.

Nora Belrose, Quintin Pope, Lucia Quirke, Alex Mallen, and Xiaoli Fern. Neural networks learn statistics of increasing complexity. *arXiv preprint arXiv:2402.04362*, 2024.

Jesse Bettencourt, Matthew J. Johnson, and David Duvenaud. Taylor-mode automatic differentiation for higher-order derivatives in JAX. In *Program Transformations for ML Workshop at NeurIPS 2019*, 2019. URL https://openreview.net/forum?id=SkxEF3FNPH.

Sid Black, Leo Gao, Phil Wang, Connor Leahy, and Stella Biderman. GPT-Neo: Large Scale Autoregressive Language Modeling with Mesh-Tensorflow, March 2021. URL https://doi.org/10.5281/zenodo.5297715. If you use this software, please cite it using these metadata.

Tolga Bolukbasi, Adam Pearce, Ann Yuan, Andy Coenen, Emily Reif, Fernanda Viégas, and Martin Wattenberg. An interpretability illusion for bert. *arXiv preprint arXiv:2104.07143*, 2021.

James Bradbury, Roy Frostig, Peter Hawkins, Matthew James Johnson, Chris Leary, Dougal Maclaurin, George Necula, Adam Paszke, Jake VanderPlas, Skye Wanderman-Milne, and Qiao Zhang. JAX: composable transformations of Python+NumPy programs, 2018. URL http://github.com/google/jax.

Thorsten Brants, Ashok Popat, Peng Xu, Franz Josef Och, and Jeffrey Dean. Large language models in machine translation. In *Proceedings of the 2007 Joint Conference on Empirical Methods in Natural Language Processing and Computational Natural Language Learning (EMNLP-CoNLL)*, pp. 858–867, 2007.

Trenton Bricken, Adly Templeton, Joshua Batson, Brian Chen, Adam Jermyn, Tom Conerly, Nick Turner, Cem Anil, Carson Denison, Amanda Askell, Robert Lasenby, Yifan Wu, Shauna Kravec, Nicholas Schiefer, Tim Maxwell, Nicholas Joseph, Zac Hatfield-Dodds, Alex Tamkin, Karina Nguyen, Brayden McLean, Josiah E Burke, Tristan Hume, Shan Carter, Tom Henighan, and Christopher Olah. Towards monosemanticity: Decomposing language models with dictionary learning. *Transformer Circuits Thread*, 2023. https://transformer-circuits.pub/2023/monosemantic-features/index.html.

Nicola Cancedda. Spectral filters, dark signals, and attention sinks, 2024.

Mary M. Comeau et al. Preventing unrestricted and unmonitored ai. *npj Digital Medicine*, 8(1):63, 2025. doi: 10.1038/s41746-025-01443-2.

Arthur Conmy, Augustine Mavor-Parker, Aengus Lynch, Stefan Heimersheim, and Adrià Garriga-Alonso. Towards automated circuit discovery for mechanistic interpretability. In A. Oh, T. Naumann, A. Globerson, K. Saenko, M. Hardt, and S. Levine (eds.), *Advances in Neural Information Processing Systems*, volume 36, pp. 16318–16352. Curran Associates, Inc., 2023. URL https://proceedings.neurips.cc/paper_files/paper/2023/file/34e1dbe95d34d7ebaf99b9bcaeb5b2be-Paper-Conference.pdf.

Charles Ehresmann. Les prolongements d'une variété différentiable: l'espace des jets d'ordre r de vn dans vm. *C. R. Acad. Sci. Paris*, 233:777–779, 1951.

Nelson Elhage, Neel Nanda, Catherine Olsson, Tom Henighan, Nicholas Joseph, Ben Mann, Amanda Askell, Yuntao Bai, Anna Chen, Tom Conerly, Nova DasSarma, Dawn Drain, Deep Ganguli, Zac Hatfield-Dodds, Danny Hernandez, Andy Jones, Jackson Kernion, Liane Lovitt, Kamal Ndousse, Dario Amodei, Tom Brown, Jack Clark, Jared Kaplan, Sam McCandlish, and Chris Olah. A mathematical framework for transformer circuits. *Transformer Circuits Thread*, 2021. https://transformer-circuits.pub/2021/framework/index.html.

Nelson Elhage, Tristan Hume, Catherine Olsson, Nicholas Schiefer, Tom Henighan, Shauna Kravec, Zac Hatfield-Dodds, Robert Lasenby, Dawn Drain, Carol Chen, Roger Grosse, Sam McCandlish, Jared Kaplan, Dario Amodei, Martin Wattenberg, and Christopher Olah. Toy models of superposition. *Transformer Circuits Thread*, 2022. https://transformer-circuits.pub/2022/toy_model/index.html.

Pablo Fernández-Becerra et al. Enhancing trust in autonomous agents: An architecture for accountability and explainability through blockchain and large language models. *arXiv preprint arXiv:2403.09567*, 2024. URL https://arxiv.org/abs/2403.09567.

Javier Ferrando and Elena Voita. Information flow routes: Automatically interpreting language models at scale. *arXiv preprint arXiv:2403.00824*, 2024.

Javier Ferrando, Gabriele Sarti, Arianna Bisazza, and Marta R Costa-jussà. A primer on the inner workings of transformer-based language models. *arXiv preprint arXiv:2405.00208*, 2024.

Samuel Gehman, Suchin Gururangan, Maarten Sap, Yejin Choi, and Noah A. Smith. RealToxicityPrompts: Evaluating neural toxic degeneration in language models. In Trevor Cohn, Yulan He, and Yang Liu (eds.), *Findings of the Association for Computational Linguistics: EMNLP 2020*, pp. 3356–3369, Online, November 2020. Association for Computational Linguistics. doi: 10.18653/v1/2020.findings-emnlp.301. URL https://aclanthology.org/2020.findings-emnlp.301.

Mor Geva, Roei Schuster, Jonathan Berant, and Omer Levy. Transformer feed-forward layers are key-value memories. In Marie-Francine Moens, Xuanjing Huang, Lucia Specia, and Scott Wen-tau Yih (eds.), *Proceedings of the 2021 Conference on Empirical Methods in Natural Language Processing*, pp. 5484–5495, Online and Punta Cana, Dominican Republic, November 2021. Association for Computational Linguistics. doi: 10.18653/v1/2021.emnlp-main.446. URL https://aclanthology.org/2021.emnlp-main.446.

Mor Geva, Avi Caciularu, Kevin Wang, and Yoav Goldberg. Transformer feed-forward layers build predictions by promoting concepts in the vocabulary space. In *Proceedings of the 2022 Conference on Empirical Methods in Natural Language Processing*, pp. 30–45, 2022.

Nicholas Goldowsky-Dill, Chris MacLeod, Lucas Sato, and Aryaman Arora. Localizing model behavior with path patching. *arXiv preprint arXiv:2304.05969*, 2023.

Joshua T Goodman. A bit of progress in language modeling. *Computer Speech & Language*, 15(4): 403–434, 2001.

Andreas Griewank and Andrea Walther. *Evaluating derivatives: principles and techniques of algorithmic differentiation*. SIAM, 2008.

Dirk Groeneveld, Iz Beltagy, Pete Walsh, Akshita Bhagia, Rodney Kinney, Oyvind Tafjord, Ananya Harsh Jha, Hamish Ivison, Ian Magnusson, Yizhong Wang, et al. Olmo: Accelerating the science of language models. *arXiv preprint arXiv:2402.00838*, 2024.

Thomas Hartvigsen, Saadia Gabriel, Hamid Palangi, Maarten Sap, Dipankar Ray, and Ece Kamar. ToxiGen: A large-scale machine-generated dataset for adversarial and implicit hate speech detection. In Smaranda Muresan, Preslav Nakov, and Aline Villavicencio (eds.), *Proceedings of the 60th Annual Meeting of the Association for Computational Linguistics (Volume 1: Long Papers)*, pp. 3309–3326, Dublin, Ireland, May 2022. Association for Computational Linguistics. doi: 10.18653/v1/2022.acl-long.234. URL https://aclanthology.org/2022.acl-long.234.

Kaiming He, Xiangyu Zhang, Shaoqing Ren, and Jian Sun. Deep residual learning for image recognition. In *Proceedings of the IEEE conference on computer vision and pattern recognition*, pp. 770–778, 2016.

Stanislaw Jastrzebski, Devansh Arpit, Nicolas Ballas, Vikas Verma, Tong Che, and Yoshua Bengio. Residual connections encourage iterative inference. *arXiv preprint arXiv:1710.04773*, 2017.

Swanand Kadhe, Long Phan, Milad Nasr, Xinyang Zhang, et al. Split, unlearn, merge: Leveraging data attributes for more effective unlearning in llms. *arXiv preprint arXiv:2406.11780*, 2024.

Jinxin Li, Tianle Wang, Yuxin Shi, Shiyu Li, et al. Editing as unlearning: Are knowledge editing methods strong baselines for large language model unlearning? *arXiv preprint arXiv:2505.19855*, 2025.

Jiacheng Liu, Sewon Min, Luke Zettlemoyer, Yejin Choi, and Hannaneh Hajishirzi. Infini-gram: Scaling unbounded n-gram language models to a trillion tokens. *arXiv preprint arXiv:2401.17377*, 2024.

X. Liu et al. A survey of large language models for healthcare. *arXiv preprint arXiv:2310.05694*, 2023. URL https://arxiv.org/abs/2310.05694.

Kevin Meng, David Bau, Alex Andonian, and Yonatan Belinkov. Locating and editing factual associations in gpt. *Advances in Neural Information Processing Systems*, 35:17359–17372, 2022.

Jack Merullo, Carsten Eickhoff, and Ellie Pavlick. Language models implement simple word2vec-style vector arithmetic. *arXiv e-prints*, pp. arXiv–2305, 2023.

Aaron Mueller. Missed causes and ambiguous effects: Counterfactuals pose challenges for interpreting neural networks. *arXiv preprint arXiv:2407.04690*, 2024.

Timothy Nguyen. Understanding transformers via n-gram statistics. *arXiv preprint arXiv:2407.12034*, 2024.

nostalgebraist. logit lens on non-gpt2 models + extensions, 2021a. URL https://colab.research.google.com/drive/1MjdfK2srcerLrAJDRaJQKO0sUiZ-hQtA.

nostalgebraist. interpreting gpt: the logit lens, 2021b. URL https://www.lesswrong.com/posts/AcKRB8wDpdaN6v6ru/interpreting-gpt-the-logit-lens#HEf5abD7hqqAY2GSQ.

Alethea Power, Yuri Burda, Harri Edwards, Igor Babuschkin, and Vedant Misra. Grokking: Generalization beyond overfitting on small algorithmic datasets, 2022.

Alec Radford, Jeff Wu, Rewon Child, David Luan, Dario Amodei, and Ilya Sutskever. Language models are unsupervised multitask learners. 2019.

George Raptis et al. Agentic llm-based robotic systems for real-world autonomous tasks: challenges and opportunities. *Frontiers in Robotics and AI*, 11, 2024. doi: 10.3389/frobt.2024.1240269.

Baptiste Rozière, Jonas Gehring, Fabian Gloeckle, Sten Sootla, Itai Gat, Xiaoqing Ellen Tan, Yossi Adi, Jingyu Liu, Romain Sauvestre, Tal Remez, Jérémy Rapin, Artyom Kozhevnikov, Ivan Evtimov, Joanna Bitton, Manish Bhatt, Cristian Canton Ferrer, Aaron Grattafiori, Wenhan Xiong, Alexandre Défossez, Jade Copet, Faisal Azhar, Hugo Touvron, Louis Martin, Nicolas Usunier, Thomas Scialom, and Gabriel Synnaeve. Code llama: Open foundation models for code, 2024.

Harshay Shah, Andrew Ilyas, and Aleksander Madry. Decomposing and editing predictions by modeling model computation. *arXiv preprint arXiv:2404.11534*, 2024.

Claude Elwood Shannon. A mathematical theory of communication. *The Bell system technical journal*, 27(3):379–423, 1948.

Helena Smith. Clinical ai: opacity, accountability, responsibility and liability. *AI & Society*, 36: 535–545, 2021. doi: 10.1007/s00146-020-01019-6.

Anej Svete and Ryan Cotterell. Transformers can represent n-gram language models. *arXiv preprint arXiv:2404.14994*, 2024.

Adly Templeton, Tom Conerly, Jonathan Marcus, Jack Lindsey, Trenton Bricken, Brian Chen, Adam Pearce, Craig Citro, Emmanuel Ameisen, Andy Jones, Hoagy Cunningham, Nicholas L Turner, Callum McDougall, Monte MacDiarmid, C. Daniel Freeman, Theodore R. Sumers, Edward Rees, Joshua Batson, Adam Jermyn, Shan Carter, Chris Olah, and Tom Henighan. Scaling monosemanticity: Extracting interpretable features from claude 3 sonnet. *Transformer Circuits Thread*, 2024. URL https://transformer-circuits.pub/2024/scaling-monosemanticity/index.html.

Hugo Touvron, Thibaut Lavril, Gautier Izacard, Xavier Martinet, Marie-Anne Lachaux, Timothée Lacroix, Baptiste Rozière, Naman Goyal, Eric Hambro, Faisal Azhar, et al. Llama: Open and efficient foundation language models. *arXiv preprint arXiv:2302.13971*, 2023a.

Hugo Touvron, Louis Martin, Kevin Stone, Peter Albert, Amjad Almahairi, Yasmine Babaei, Nikolay Bashlykov, Soumya Batra, Prajjwal Bhargava, Shruti Bhosale, et al. Llama 2: Open foundation and fine-tuned chat models. *arXiv preprint arXiv:2307.09288*, 2023b.

Ashish Vaswani, Noam Shazeer, Niki Parmar, Jakob Uszkoreit, Llion Jones, Aidan N Gomez, Łukasz Kaiser, and Illia Polosukhin. Attention is all you need. *Advances in neural information processing systems*, 30, 2017.

Andreas Veit, Michael J Wilber, and Serge Belongie. Residual networks behave like ensembles of relatively shallow networks. *Advances in neural information processing systems*, 29, 2016.

Elena Voita, Javier Ferrando, and Christoforos Nalmpantis. Neurons in large language models: Dead, n-gram, positional. In Lun-Wei Ku, Andre Martins, and Vivek Srikumar (eds.), *Findings of the Association for Computational Linguistics ACL 2024*, pp. 1288–1301, Bangkok, Thailand and virtual meeting, August 2024. Association for Computational Linguistics. URL https://aclanthology.org/2024.findings-acl.75.

Sandra Wachter, Brent Mittelstadt, and Luciano Floridi. Transparent, explainable, and accountable ai for robotics. In *Proceedings of IJCAI Workshop on Explainable Artificial Intelligence*, 2017. URL https://www.researchgate.net/publication/318819126_Transparent_Explainable_and_Accountable_AI_for_Robotics.

Kevin Wang, Alexandre Variengien, Arthur Conmy, Buck Shlegeris, and Jacob Steinhardt. Interpretability in the wild: a circuit for indirect object identification in gpt-2 small. *arXiv preprint arXiv:2211.00593*, 2022.

Xiangxiang Xu, Shao-Lun Huang, Lizhong Zheng, and Gregory W Wornell. An information theoretic interpretation to deep neural networks. *Entropy*, 24(1):135, 2022.

Xueliang Xu, Haoyue Wang, Bowen Yu, Dongyan Zhao, and Rui Yan. Reasoning based on symbolic and parametric knowledge. *arXiv preprint arXiv:2501.01030*, 2025.

Chiyuan Zhang, Samy Bengio, Moritz Hardt, Benjamin Recht, and Oriol Vinyals. Understanding deep learning (still) requires rethinking generalization. *Communications of the ACM*, 64(3):107–115, 2021.

Honghua Zhang, Meihua Dang, Nanyun Peng, and Guy Van den Broeck. Tractable control for autoregressive language generation. In *International Conference on Machine Learning*, pp. 40932–40945. PMLR, 2023.

A ADDITIONAL DETAILS ON JETS

A jet of a function represents an equivalence class. We thus can perform algebraic operations among functional equivalence classes using jet algebra stated below.

Proposition 1 (Jet algebra). *Let $f, g \in C^\infty(\mathbb{R}^d, \mathbb{R}^d)$ and $k \in \mathbb{N}^+$. Then,*

(i) $\mathrm{J}^k(af + bg)(x_0) = a\,\mathrm{J}^k(f)(x_0) + b\,\mathrm{J}^k(g)(x_0)$*, for $a, b \in \mathbb{R}$ (linearity);*

(ii) $\mathrm{J}^k f(x_0) \circ g \in \mathrm{J}^k f(x_0)$ *and* $\mathrm{J}^k f(x_0) \circ g(y) = \mathrm{J}^k f(x_0)(g(y))$ *(jet after endomorphisms);*

(iii) $g \circ \mathrm{J}^k f(x_0) = \{g \circ u : u \in \mathrm{J}^k f(x)\}$ *(endomorphism after jet);*

(iv) $\mathrm{J}^k(f \circ g)(x_0) = \mathrm{J}^k f(g(x)) \circ \mathrm{J}^k g(x_0)$ *(composition of jets);*

Properties *(i)-(iii)* follow directly from the definition; *(iv)* is a consequence of the chain rule and truncation.

Proof of Lemma 1 Take $y \in \mathbb{R}^d$, $N \geq 1$, $x_i \in \mathbb{R}^d$ for $i \in [N]$, $w \in \triangle^{N-1}$ and an order $k \geq 0$. Since w belongs to the simplex $\triangle^{N-1}$, we have $\sum_{i=1}^N w_i = 1$. Multiplying $f(y)$ on both hands, we obtain

$$f(y) = \sum_{i=1}^N w_i f(y) = \sum_{i=1}^N w_i \left[f(x_i) + \sum_{s=1}^k \mathrm{D}^s f(x_i)(y - x_i)^{\otimes s} + O(\|y - x_i\|^{k+1}) \right]$$
$$= \sum_{i=1}^N w_i \mathrm{J}^k f(x_i)(x) + O(w_i \|y - x_i\|^{k+1}),$$

by applying eq. (3) (Taylor expansion) and the definition of jet with each x_i as the center. At the same time, we can expand $f(y)$ with $\sum_{i=1}^N x_i$ as the center

$$f(y) = \mathrm{J}^k f(\sum_{i=1}^N x_i)(x) + O(\|y - \sum x_i\|^{k+1}).$$

Now let us take $y = \sum_{i=1}^N x_i$ and observe that $O(\|y - \sum x_i\|^{k+1}) = 0$ and $O(w_i \|y - x_i\|^{k+1}) = O(w_i \|x_i - \sum_j x_j\|^{k+1})$. Finally we observe that the class of functions in the last O are dominated by the class of function in $O(r^{k+1})$ where $r = \max_i\{w_i \|x_i - \sum_j x_j\|\}$ is the maximum remainder. This concludes the proof.

As a side note, jet weights would not need to form convex combinations, but rather linear combinations $\sum_i w_i = 1$. However, restricting to convex combinations has two major advantages:

- optimizing over a convex set guarantees the existence of maxima and minima (Weierstrass theorem) and uniqueness of minima if we are optimizing a strictly convex loss as in general is the case for expansions that only affect the decoder module.
- weights within the probability simplex have a clearer interpretation for interpretability purposes.

B ADDITIONAL DETAILS ON RUNTIME

We report in fig. 5 a plot of the runtime for evaluating expansions originating from the joint jet lenses of section 5.2.1 as a ratio of the input model evaluation (forward pass), for both the uniform and the optimized jet weights w setup, for different jet orders k.

C ADDITIONAL DETAILS ON JET n-GRAMS

General concept of n-gram models The general concept of n-gram models linked to (transformer-based) LMs involves defining or constructing mappings that functionally depend only on $n - 1$ input tokens (with the n-th token being the output token) to capture and describe the behaviour of the original LM. We are not the first to explore this idea; for instance Nguyen (2024) fits n-grams on the same dataset used to train the LM.

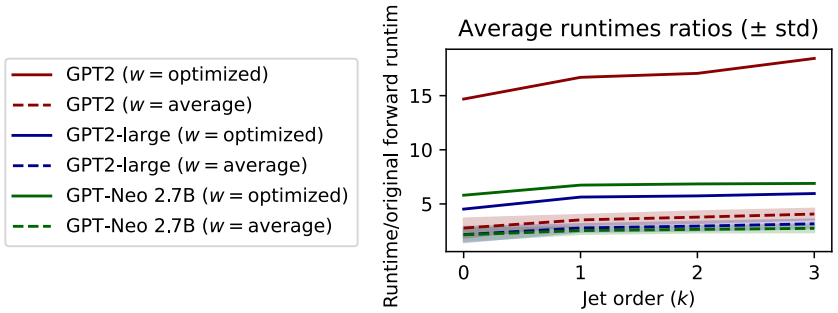

Figure 5: Empirical runtime of evaluations of jet expansions originating form the joint jet lenses as a ratio of the evaluation of the input model.

Jet expansions for in-model n-Grams Jet expansions allow us to define n-grams statistics that are derived solely and directly from the model itself – producing in-model n-grams rather than in-data n-grams. This approach offers at least two significant advantages:

- **No Dataset Preparation:** It eliminates the need for dataset preparation to collect activation patterns when interpreting the model globally, thereby saving time and computational resources. This process can be conducted entirely on CPU, which is approximately 10 times cheaper per hour compared to GPUs in the current market.
- **Avoidance of Fitting Artifacts:** It avoids potential artifacts that could arise from the selection of external n-gram fitting methods.

We describe the detailed relationship between the bi-gram/tri-gram, which we used in our case studies, and the jet expansion as follows.

Jet bi-Grams Jet bi-grams are paths that do not pass through self-attention layers. In experiments, we focus on two types of bi-gram paths. a) the embedding-unembedding path that can be obtained as jet_expand$(f, L, \{\text{Enc}\}, 0)$. b) paths that pass through one MLP module, assuming MLPs are at odd block indices in the residual network architecture, the procedure to extract the path is:

$$
\begin{aligned}
&\mathcal{C} = \{\text{Enc}\} \\
&\text{for } l = 1, 3, \ldots, L-1: \\
&\quad \xi, \delta = \text{jet\_expand}(f, l, \{\text{Enc}\}, 0) \\
&\quad \mathcal{C} = \mathcal{C} \cup \{e(\cdot, 1)\}_{e \in \xi} \\
&\quad \xi, \delta = \text{jet\_expand}(f, L, \mathcal{C}, 0)
\end{aligned}
$$

This procedure results in a series of functions in ξ—one for each MLP layer—that depend only on the last input token. Applying softmax normalization to their logit output allows these functions to define (conditional) bi-grams. Similar constructions can be performed for paths through multiple MLPs. We will release code for these procedures and also provide equivalent algorithms that directly use transformer modules.

Jet tri-Grams Jet tri-grams involve paths that pass through at least one self-attention layer, with a need to isolate the contribution from the first token of the tri-gram. The procedure for extracting a 0-th order jet trigram path that passes through the ith self-attention layer (assuming it has one head and σ_2 is a function that extracts the last two tokens from a sequence of length at least 2) is as follows:

$$
\begin{aligned}
&\text{Define} \quad \sigma_2(z) = (z_{t-1}, z_t) \\
&\text{Compute} \quad \xi, \delta = \text{jet\_expand}(f, i, \{\text{Enc} \circ \sigma_2\}, 0) \\
&\text{Compute} \quad \xi, \delta = \text{jet\_expand}(f, L, \{e(\cdot, 1)\}_{e \in \xi}, 0)
\end{aligned}
$$

This procedure yields a map that depends only on two input tokens, isolating the contribution of the ith self-attention layer on pairs of tokens. Once softmax normalization is applied, this defines a tri-gram. The tri-gram could represent either a skip trigram or a contiguous trigram, depending on how positional information is encoded (e.g., absolute positional embeddings versus rotary embeddings).

D ADDITIONAL DETAILS ON THE EXPERIMENTAL METRICS

Δ logit after intervention To compute Δ logits, we calculate the logits for the given n-gram both before and after applying the intervention, then determine the change in the logits. For example, consider the trigram (Lemma, let, s). We compute the logit of "s" conditioned on the input "Lemma let". The intervention involves removing the corresponding attention head (e.g., head 2). We then measure and report the change in the logit for "s" as a result of this intervention.

One-to-one bi-grams like and many-to-many bi-grams One-to-one bi-bigrams are (approximately) unimodal bi-grams that concentrate all mass on a single token: i.e. given z_1, $\mathbb{P}\_\mathcal{D}(z_2|z_1) \approx 1$ and given z_2, $\mathbb{P}_\mathcal{D}(z_1|z_2) \approx 1$ for a specific pair of token and close to 0 for all others. In the example in the paper, $z_1 =$ "&", and $z_2 =$ "amp". $\mathbb{P}_\mathcal{D}$ is the probability distribution induced by the pre-training data. Many-to-many bi-grams we refer to the opposite scenario where both the conditional probabilities are highly multi-modal. In the example $z_1 =$"make" and $z_2 =$"sure" we have that many other tokens can succeed $z_1 =$"make" or precede $z_2 =$"sure".

Hit ratios of bi-grams The Hit Ratio (HR@n), often referred to as hit rate, is a metric commonly used in ranking tasks. In our context, we treat each checkpoint of the language model as a "ranker" of bigrams. The Hit Ratio measures how effectively the current model checkpoint retrieves high-quality bigrams from the set of all possible bigrams. To quantify the model's progress, we define the bigrams at the final step as the "good" bigrams and measure how quickly the model approaches these high-quality bigrams. Specifically, we compute the HR@n to evaluate how often the model's output bigrams match those in the "true" top n ranked bi-grams given by the final step. Formally, the Hit Ratio@n is given by

$$\text{HR@}n = \frac{1}{n}\sum_{i=1}^{n} \mathbb{I}(\text{the i-th bigram output by the current model} \in \text{True\_Top\_n})$$

where n is the number of top predictions being considered and

- $\mathbb{I}$ is the indicator function that returns 1 if the i-th bigram output by the model is present in the True Top n bigrams, and 0 otherwise,
- True_Top_n represents the set of "good" bigrams, which in our case is the set of the top n scoring bigrams from the final model step.

Total mass of bi-grams We use the total mass as a metric to measure the cumulative probabilities of bi-grams from the top 1K bi-grams, weighted by an empirical unigram distribution derived from real data. Formally, it is given by: Total Mass $= \sum_{(z_1,z_2)\in\text{Top-1K}} \mathbb{P}_{e_t}(z_2|z_1)\mathbb{P}_\mathcal{D}(z_1)$ where:

- e_t is the embedding-unembedding path at the t-th pre-training step,
- (z_1, z_2) are the bigrams being considered,
- $\mathbb{P}_{e_t}(z_2|z_1)$ is the probability assigned by the model e_t (the embedding-unembedding path) for the token z_2 given token z_1,
- $\mathbb{P}_\mathcal{D}(z_1)$ is the probability of z_1 under the empirical distribution $\mathcal{D}$, which is the unigram probability given by the Infini-gram API (**?**) on the Dolma dataset (**?**) (the dataset used to pretrain the model checkpoints).

This metric is designed to evaluate how much "correct" probability mass the model checkpoints assign to bigrams (z_1, z_2), taking into account the empirical unigram probability of z_1. It provides insight into how well the model aligns with the empirical distribution of real-world data during the pretraining process.

E ADDITIONAL DETAILS ON JET n-GRAM DIFFING

We derive the top-K bi-grams for each model from their embedding-unembedding path, which can be obtained as jet_expand$(f, L, \{\text{Enc}\}, 0)$. These bigrams are then saved into CSVs, allowing us to represent models via their respective bigram files. By comparing these files directly, much like comparing text files, we bypass the challenges of comparing the models in the parameter space, where measuring behavioral-level differences can be difficult. For example, we extract the bigram files for Llama-2-7B, and its coding finetuned versions. In summary, by transforming models into bigram files (Model $\rightarrow$ Bigram File), we can effectively compare their behavior via bigram file differences (Model Diff $\rightarrow$ Bigram File Diff). We will include a demonstration in supplementary material.

F ADDITIONAL ANALYSIS INTO THE BI-GRAMS PRETRAINING DYNAMICS

Pretraining an LLM is usually extremely resource intensive. Therefore it is crucial to monitor the progress of a pretraining run to prevent wasting of time and compute. In this section, we show how jet bi-grams can serve as an effective signaling tool to trace the pretraining dynamics, providing insights about the model's maturity. Such signals are especially useful to understand what happens with the model when the pretraining loss shows marginal improvements and fails to reflect the changes inside the model.

Identifying the top bi-grams. To assess the model's progression, we extracted jet bi-grams from *OLMo-7B* model checkpoints across 555K pretraining steps. Table 5 presents a summary of the top 10 jet bi-grams at different stages of training. Due to space reason, we only show the top 10 jet bi-grams every 100K steps. Initially, the network exhibits nonsensical jet bi-grams, such as "`ICUirling`". As training advances, it gradually learns more meaningful combinations, like "`at least`". This process of acquiring sensible bi-grams stabilizes around step 200K, indicating that the model is reaching a level of maturity where the top 10 bi-grams capture common meaning.

Learning speed. To evaluate the learning speed of jet bi-grams during pretraining, we consider the jet bi-grams at the final training step (555K) as the ground-truth bi-grams. We then chart the hit ratios of these ground-truth bi-grams at each pretraining step, as illustrated in Figure 7a. Interestingly, even though the pretraining loss (the blue curve) shows only minor improvements after the initial 50K steps, the model's acquisition of effective bi-grams continues to progress in a steady, consistent manner. Hence bi-grams learning dynamics are active throughout the training procedure, even after the training loss stabilizes. This indicates that there is significant behavior change in the model which is not well captured by the training loss, an observation that is studied also in grokking and double-descent (Zhang et al., 2021; Power et al., 2022). In other words, jet bi-grams may offer another point of view for analyzing the learning dynamics compared to pretraining loss. In addition, fig. 7b characterizes the total pseudo-joint probability mass of top 1K bi-grams from empirical data (Liu et al., 2024). We derive a pseudo-joint jet bi-gram probability using statistical uni-grams from (Liu et al., 2024). We observe that the model gradually accumulates probability mass that aligns with the real corpus data distribution.

Learning schemes for different bi-grams. To understand if there are any differences between the learning schemes of different bi-grams, we can trace the progression of the jet bi-gram scores for selected bi-grams. Figure 6 provides a visual comparison of how different bi-grams are promoted or suppressed during the pretraining process. The different slopes and levels of the lines indicate varying rates of learning for the respective bi-grams. We observe that, the model first acquires random bi-grams due to random parameter initialization. These random bi-grams, like "`ICUirling`" and "`VENT thanks`", are quickly suppressed in the early steps and never regain high scores. In contrast, one-to-many bi-grams like "`at least`" are first promoted to very high scores but then get suppressed perhaps due to the model seeing more of the scope of the token "at". One-to-one bi-grams like "`&amp`" (HTML code) are gradually promoted and stabilize. Many-to-many bi-grams like "`make sure`" takes the most time to learn and the scores are still increasing even at the end of pretraining. Our findings suggest that the training process effectively promotes certain "good" bi-grams, but at different paces, where they might be suppressed later depending on their occurrences and linguistic nature. These insights could inform future training strategies, such as targeted training on more relevant bi-grams or adjusting the training data to improve the pretraining speed.

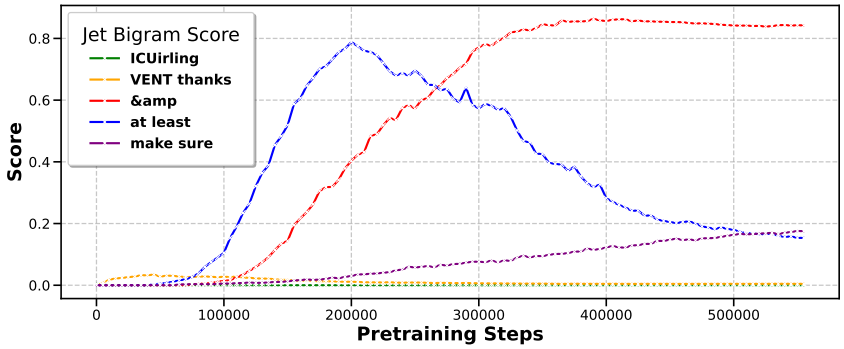

Figure 6: Visualization of *OLMo-7B*'s promotion and suppression dynamics of jet bi-grams scores.

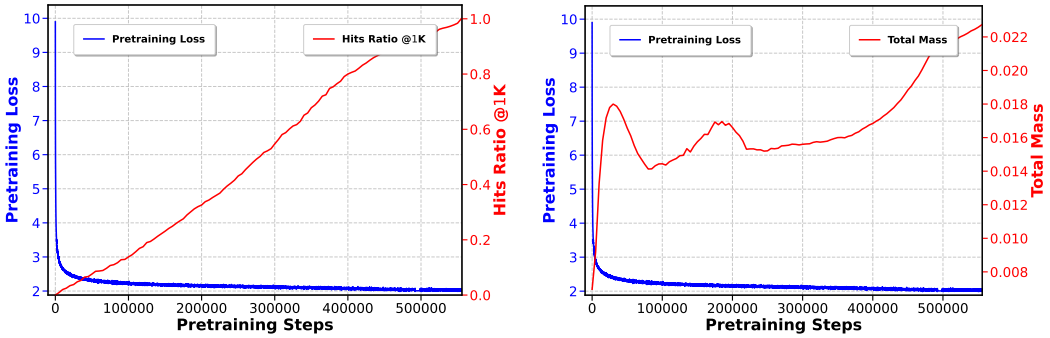

(a) Top 1K jet bi-gram hit ratios w.r.t. the final step.

(b) Top 1K jet bi-gram mass w.r.t. empirical data.

Figure 7: Analysis of *OLMo-7B*'s pretraining dynamics via measuring its jet bi-gram progression.

G Additional tables for Jet Bi-grams

See table 5 and table 3.

H Additional tables for Jet Paths

Table 6 reports a role identification study on attention heads in the first self-attention of *OLMo-7B* using jet tri-grams. Specifically, we find heads associated with math and programming, e.g. head 1 on Math/Latex; heads promoting digits and dash composition into dates, e.g. head 25; and heads constituting phrase templates, e.g. head 15 managing a "for x purposes", where x is a placeholder. To verify the roles we revealed, we further perform preliminary intervention experiments where we ablate MLPs or attention heads and compute variations in model logits. After the interventions, the logits drop consistently in all cases, suggesting our jet n-grams indeed can help identify certain roles for selected components. Varying impact on logit differences is likely due to overdetermination

Table 5: Bi-gram evolution across pretraining steps for OLMo 7B. Each column represents a distinct step, while each row corresponds to a different rank. The table entries are the bi-grams at each step for each rank. The number of tokens seen in association with the pretraining steps is also annotated. The model gradually picks up meaningful bi-grams after starting from senseless bi-grams (due to random initialization).

Rank	0K [#steps] 0B [#tokens]	100K 442B	200K 885B	300K 1327B	400K 1769B	555K 2455B
0	immortal	's	at least	&amp	&amp	&amp
1	ICUirling	at least	's	at least	its own	its own
2	ords architect	its own	&amp	its own	their own	their own
3	yaml Adam	okerly	your own	your own	at least	his own
4	231 next	VENT thanks	its own	their own	your own	make sure
5	clonal	iums	iums	more than	his own	your own
6	Charg@{	you're	you're	can't	2nd	2nd
7	avoir careless	Everything v	2nd	his own	more than	at least
8	HOLD worsening	erna already	you guys	2nd	make sure	more than
9	Horse dismant	'my	more than	make sure	can't	iums

Table 6: Several attention heads in the first residual block of *OLMo-7B* and their roles identified with jet tri-grams extracted from corresponding jet paths. We also include an example tri-gram captured by each head.

Head Index	2	16	26	30
Role	Math/LaTeX	"for . . . purposes"	date composition	"into account/consideration . . . "
Example 3-gram	`(_Lemma, _let, _s)`	`(_for, _use, _purposes)`	`(20, 23, _-)`	`(_into, _account, _possible)`
Δlogit after intervention	−0.1570	−0.0019	−0.0093	−0.0001

	new	simple	neural	architecture	,	the	Trans	former
Block 1	Supporters	Supporters	Supporters	Supporters	Supporters	Supporters	Supporters	Supporters
Block 2	Supporters	Supporters	Supporters	Supporters	Supporters	Supporters	Supporters	Supporters
Block 3	Supporters	Supporters	Supporters	Supporters	Supporters	Supporters	Supporters	Supporters
Block 4	Supporters	Supporters	Supporters	Supporters	Supporters	Supporters	Supporters	Supporters
Block 5	Supporters	Supporters	Supporters	Supporters	Supporters	Supporters	Supporters	Supporters
Block 6	Supporters	Supporters	Supporters	Supporters	Supporters	Supporters	Supporters	Supporters
Block 7	Supporters	Supporters	Supporters	Supporters	Supporters	Supporters	Supporters	Supporters
Block 8	Supporters	Supporters	Supporters	Supporters	Supporters	Supporters	Supporters	Supporters
Block 9	Supporters	Supporters	Supporters	Supporters	Supporters	Supporters	Supporters	Supporters
Block 10	Supporters	Supporters	Supporters	Supporters	Supporters	Supporters	Supporters	Supporters
Block 11	Supporters	Supporters	Supporters	Supporters	Supporters	Supporters	Supporters	Supporters
Block 12	Supporters	Supporters	Supporters	Supporters	Supporters	Supporters	Supporters	Supporters
Block 13	Supporters	Supporters	Supporters	Supporters	Supporters	Supporters	Supporters	Supporters
Block 14	Supporters	Supporters	Supporters	Supporters	Supporters	Supporters	Supporters	Supporters
Block 15	Supporters	Supporters	Supporters	Supporters	Supporters	Supporters	Supporters	Supporters
Block 16	Supporters	Supporters	Supporters	Supporters	Supporters	Supporters	Supporters	Supporters
Block 17	Supporters	Supporters	Supporters	Supporters	Supporters	Supporters	Supporters	Supporters
Block 18	Supporters	Supporters	Supporters	Supporters	Supporters	Supporters	Supporters	Supporters
Block 19	Supporters	Supporters	Supporters	Supporters	Supporters	Supporters	Supporters	Supporters
Block 20	Supporters	Supporters	Supporters	Supporters	Supporters	Supporters	Supporters	Supporters
Block 21	Supporters	Supporters	Supporters	Supporters	Engineers	Supporters	Supporters	Supporters
Block 22	Supporters	Supporters	Supporters	Supporters	Supporters	Supporters	Supporters	Introduced
Block 23	Supporters	Supporters	Supporters	Supporters	Introduced	Supporters	Supporters	Introduced
Block 24	Supporters	Supporters	Supporters	Supporters	Nonetheless	Nonetheless	Supporters	Introduced
Block 25	Supporters	Supporters	Supporters	Supporters	Attempts	Nonetheless	Supporters	Introduced
Block 26	Supporters	Supporters	Supporters	Supporters	Attempts	Nonetheless	Introduced	Introduced
Block 27	Supporters	Supporters	Supporters	Supporters	Attempts	Nonetheless	Introduced	Introduced
Block 28	Supporters	Supporters	Supporters	Supporters	Attempts	Nonetheless	Introduced	Introduced
Block 29	foreseen	Supporters	Supporters	Supporters	foreseen	Nonetheless	Charges	Introduced
Block 30	foreseen	Supporters	Supporters	Attempts	foreseen	foreseen	Charges	Introduced
Block 31	Supporters	Supporters	Supporters	_for	_the	aminer	former	,
Block 32	_	_	_network	_for	_which	_neural	former	,
Logits	_	_	_network	_for	_which	_neural	former	,

Figure 8: Iterative jet lens ($k = 0$), equivalent to logit lens(nostalgebraist, 2021b), applied over GPT-Neo-2.7B with the input sentence "new simple neural architecture, the Transformer".

(Mueller, 2024) and our partial selection of jet paths (e.g. for tri-grams we only selected encoding-attention-decoding paths, excluding any MLP).

I Additional plots of jet lenses

See plots below, referring to the main paper for details. Note that for iterative lenses the last block coincides with the model logits for all k by design. We omit the iterative lens for GPT2-large for $k = 2$ due to low cosine similarity.

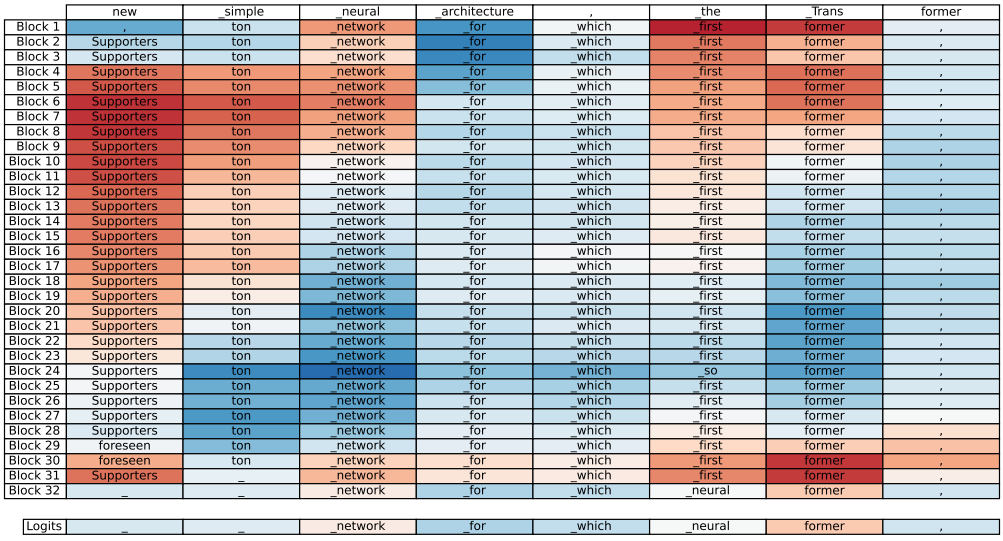

	new	_simple	_neural	_architecture	,	_the	_Trans	former
Block 1	,	ton	_network	_for	_which	_first	former	,
Block 2	Supporters	ton	_network	_for	_which	_first	former	,
Block 3	Supporters	ton	_network	_for	_which	_first	former	,
Block 4	Supporters	ton	_network	_for	_which	_first	former	,
Block 5	Supporters	ton	_network	_for	_which	_first	former	,
Block 6	Supporters	ton	_network	_for	_which	_first	former	,
Block 7	Supporters	ton	_network	_for	_which	_first	former	,
Block 8	Supporters	ton	_network	_for	_which	_first	former	,
Block 9	Supporters	ton	_network	_for	_which	_first	former	,
Block 10	Supporters	ton	_network	_for	_which	_first	former	,
Block 11	Supporters	ton	_network	_for	_which	_first	former	,
Block 12	Supporters	ton	_network	_for	_which	_first	former	,
Block 13	Supporters	ton	_network	_for	_which	_first	former	,
Block 14	Supporters	ton	_network	_for	_which	_first	former	,
Block 15	Supporters	ton	_network	_for	_which	_first	former	,
Block 16	Supporters	ton	_network	_for	_which	_first	former	,
Block 17	Supporters	ton	_network	_for	_which	_first	former	,
Block 18	Supporters	ton	_network	_for	_which	_first	former	,
Block 19	Supporters	ton	_network	_for	_which	_first	former	,
Block 20	Supporters	ton	_network	_for	_which	_first	former	,
Block 21	Supporters	ton	_network	_for	_which	_first	former	,
Block 22	Supporters	ton	_network	_for	_which	_first	former	,
Block 23	Supporters	ton	_network	_for	_which	_first	former	,
Block 24	Supporters	ton	_network	_for	_which	_so	former	,
Block 25	Supporters	ton	_network	_for	_which	_first	former	,
Block 26	Supporters	ton	_network	_for	_which	_first	former	,
Block 27	Supporters	ton	_network	_for	_which	_first	former	,
Block 28	Supporters	ton	_network	_for	_which	_first	former	,
Block 29	foreseen	ton	_network	_for	_which	_first	former	,
Block 30	foreseen	ton	_network	_for	_which	_first	former	,
Block 31	Supporters	_	_network	_for	_which	_first	former	,
Block 32	_	_	_network	_for	_which	_neural	former	,
Logits	_	_	_network	_for	_which	_neural	former	,

Figure 9: Iterative jet lens ($k = 1$), applied over GPT-Neo-2.7B with the input sentence "new simple neural architecture, the Transformer"

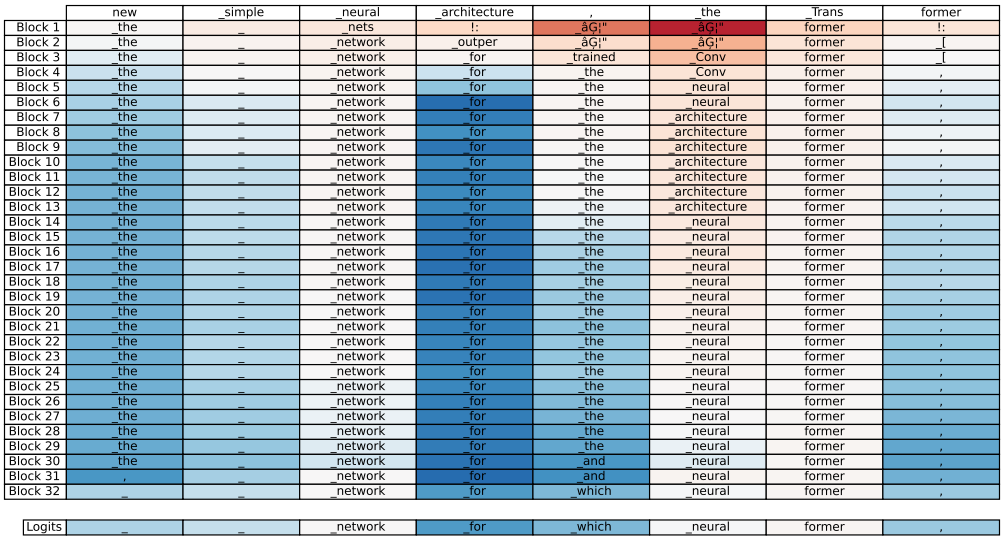

	new	_simple	_neural	_architecture	,	_the	_Trans	former
Block 1	_the	_	_nets	!:	_âĢ¦"	_âĢ¦"	former	!:
Block 2	_the	_	_network	_outper	_âĢ¦"	_âĢ¦"	former	_[
Block 3	_the	_	_network	_for	_trained	_Conv	former	_[
Block 4	_the	_	_network	_for	_the	_Conv	former	,
Block 5	_the	_	_network	_for	_the	_neural	former	,
Block 6	_the	_	_network	_for	_the	_neural	former	,
Block 7	_the	_	_network	_for	_the	_architecture	former	,
Block 8	_the	_	_network	_for	_the	_architecture	former	,
Block 9	_the	_	_network	_for	_the	_architecture	former	,
Block 10	_the	_	_network	_for	_the	_architecture	former	,
Block 11	_the	_	_network	_for	_the	_architecture	former	,
Block 12	_the	_	_network	_for	_the	_architecture	former	,
Block 13	_the	_	_network	_for	_the	_architecture	former	,
Block 14	_the	_	_network	_for	_the	_neural	former	,
Block 15	_the	_	_network	_for	_the	_neural	former	,
Block 16	_the	_	_network	_for	_the	_neural	former	,
Block 17	_the	_	_network	_for	_the	_neural	former	,
Block 18	_the	_	_network	_for	_the	_neural	former	,
Block 19	_the	_	_network	_for	_the	_neural	former	,
Block 20	_the	_	_network	_for	_the	_neural	former	,
Block 21	_the	_	_network	_for	_the	_neural	former	,
Block 22	_the	_	_network	_for	_the	_neural	former	,
Block 23	_the	_	_network	_for	_the	_neural	former	,
Block 24	_the	_	_network	_for	_the	_neural	former	,
Block 25	_the	_	_network	_for	_the	_neural	former	,
Block 26	_the	_	_network	_for	_the	_neural	former	,
Block 27	_the	_	_network	_for	_the	_neural	former	,
Block 28	_the	_	_network	_for	_the	_neural	former	,
Block 29	_the	_	_network	_for	_the	_neural	former	,
Block 30	_the	_	_network	_for	_and	_neural	former	,
Block 31	,	_	_network	_for	_and	_neural	former	,
Block 32	_	_	_network	_for	_which	_neural	former	,
Logits	_	_	_network	_for	_which	_neural	former	,

Figure 10: Iterative jet lens ($k = 2$), applied over GPT-Neo-2.7B with the input sentence "new simple neural architecture, the Transformer"

	new	_simple	_neural	_architecture	,	_the	_Trans	former
Block 1	bie	_simple	_neural	_architecture	_and	_the	fig	former
Block 2	bie	_simple	_neural	_architecture	_and	_main	ient	former
Block 3	bie	_simple	_neural	_architecture	_and	_new	ient	former
Block 4	bie	_way	_neural	_architecture	_and	_first	ient	_titan
Block 5	bie	_way	_networks	_architecture	_and	_next	ient	_Prime
Block 6	bie	_enough	_networks	_architecture	_and	_next	ient	_Matrix
Block 7	_href	_enough	_networks	_architecture	_and	_first	ient	_Prime
Block 8	_iTunes	_enough	_neural	_architecture	_which	_first	ient	_Revolution
Block 9	,	_enough	_neural	_architecture	_which	_first	ient	_Prime
Block 10	,	_enough	_network	_architecture	_which	_first	ient	_Revolution
Block 11	,	_enough	_network	_model	_which	_only	ient	_Pro
Block 12	,	_enough	_network	_architecture	_which	_only	ient	_Pro
Block 13	,	_enough	_network	_model	_which	_first	ient	_Pro
Block 14	,	_enough	_network	_model	_which	_first	ient	_Pro
Block 15	,	_enough	_network	_model	_which	_only	ient	_Pro
Block 16	,	-	_network	_model	_which	_only	ient	_Revolution
Block 17	,	-	_system	_model	_which	_only	ient	_Prime
Block 18	,	-	_system	_model	_which	_only	ient	_Prime
Block 19	,	-	_system	_model	_which	_only	ient	_Prime
Block 20	,	-	_system	_model	_which	_only	ient	_Prime
Block 21	,	-	_system	_model	_which	_only	ient	_Prime
Block 22	,	-	_network	_model	_which	_only	ient	_Prime
Block 23	,	ton	_network	_model	_which	_only	ient	_Prime
Block 24	,	ton	_network	_model	_which	_only	ient	_Prime
Block 25	,	ton	_network	_model	_which	_first	ient	_Prime
Block 26	,	ton	_network	_model	_which	_only	ient	_Prime
Block 27	,	ton	_network	_for	_which	_first	ient	_Prime
Block 28	,	-	_network	"	_which	_only	ient	_Prime
Block 29	,	-	_network	"	_which	_neural	ient	_Prime
Block 30	,	"	_network	"	_which	_neural	ient	,
Block 31	,	"	_network	"	_which	_neural	ient	,
Block 32	,	"	_network	"	_which	_neural	ient	,
Block 33	,	"	_network	_for	_which	_neural	ient	,
Block 34	,	"	_network	'	_which	_neural	ient	,
Block 35	,	"	_network	'	_which	_neural	c	,
Block 36	_	"	_network	'	_which	_neural	c	,
Logits	_	"	_network	'	_which	_neural	c	,

Figure 11: Iterative jet lens ($k = 0$), equivalent to logit lens(nostalgebraist, 2021b), applied over GPT-2-large with the input sentence "new simple neural architecture, the Transformer".

	new	_simple	_neural	_architecture	,	_the	_Trans	former
Block 1	bie	"	_network	"	_which	_neural	c	_is
Block 2	bie	"	_network	'	_which	_neural	c	_is
Block 3	bie	"	_network	'	_which	_neural	c	_is
Block 4	_	"	_network	'	_which	_neural	c	_is
Block 5	_	"	_network	'	_which	_neural	c	_is
Block 6	_	"	_network	'	_which	_neural	c	_is
Block 7	_	"	_network	'	_which	_neural	c	_is
Block 8	_	"	_network	'	_which	_neural	c	_is
Block 9	_	"	_network	'	_which	_neural	c	_is
Block 10	,	"	_network	'	_which	_neural	c	_is
Block 11	,	"	_network	'	_which	_neural	c	_is
Block 12	,	"	_network	'	_which	_neural	c	,
Block 13	,	"	_network	'	_where	_neural	c	,
Block 14	,	"	_network	'	_and	_neural	c	,
Block 15	,	"	_network	'	_and	_neural	c	,
Block 16	,	"	_network	'	_and	_neural	c	,
Block 17	,	"	_network	'	_and	_neural	c	,
Block 18	,	"	_network	'	_and	_neural	c	,
Block 19	,	"	_network	'	_and	_neural	c	,
Block 20	,	"	_network	'	_and	_neural	c	,
Block 21	,	"	_network	'	_and	_neural	c	,
Block 22	,	"	_network	'	_and	_neural	c	,
Block 23	,	"	_network	'	_the	_neural	c	,
Block 24	,	"	_network	'	_and	_neural	c	,
Block 25	,	"	_network	'	_and	_neural	c	,
Block 26	,	"	_network	'	_and	_neural	c	,
Block 27	,	"	_network	'	_and	_neural	c	,
Block 28	,	"	_network	'	_and	_neural	c	,
Block 29	,	"	_network	'	_and	_human	c	,
Block 30	,	"	_network	'	_and	_same	c	,
Block 31	,	"	_network	'	_and	_same	c	,
Block 32	,	"	_network	'	_and	_same	c	,
Block 33	,	"	_network	'	_and	_neural	c	,
Block 34	,	"	_network	'	which	_neural	c	,
Block 35	-	"	_network	'	which	_neural	c	,
Block 36	_	"	_network	'	which	_neural	c	,
Logits	_	"	_network	'	_which	_neural	c	,

Figure 12: Iterative jet lens ($k = 1$), applied over GPT-2-large with the input sentence "new simple neural architecture, the Transformer"

	new	_simple	_neural	_architecture	,	_the	_Trans	former
Block 1 (4.40%)	, (6.62%)	_simple (3.91%)	_neural (4.42%)	_architecture (3.97%)	_which (4.07%)	_same (4.37%)	cend (3.93%)	former (3.91%)
Block 2 (4.15%)	, (6.59%)	_retro (3.85%)	_prog (4.32%)	_error (3.74%)	_including (3.93%)	_resulting (4.14%)	ference (3.69%)	_Robo (2.99%)
Block 3 (4.23%)	, (6.59%)	ove (4.13%)	_Matter (4.12%)	killer (3.51%)	_which (4.00%)	_AVG (4.01%)	em (3.56%)	Mars (3.91%)
Block 4 (4.11%)	_the (6.59%)	_reg (3.51%)	lect (4.37%)	OX (3.68%)	_found (4.05%)	netflix (4.09%)	Charge (2.95%)	Ã® (3.69%)
Block 5 (6.11%)	, (6.59%)	ware (3.54%)	_product (3.68%)	_towards (3.70%)	_evolution (3.88%)	_ones (3.74%)	it (20.20%)	_Mant (3.57%)
Block 6 (3.91%)	, (6.58%)	ies (3.59%)	_networks (4.11%)	_developed (3.45%)	_developed (3.55%)	_Mehran (3.45%)	ition (3.54%)	bur (3.01%)
Block 7 (4.00%)	, (6.56%)	face (3.75%)	_studies (3.88%)	_based (3.52%)	_hackers (3.76%)	_Turing (3.73%)	_Series (2.97%)	_Suite (3.83%)
Block 8 (4.06%)	, (6.42%)	key (3.83%)	_model (4.18%)	_based (3.53%)	_requiring (3.49%)	_algorithm (4.14%)	ient (3.62%)	_II (3.25%)
Block 9 (4.09%)	, (7.45%)	_clutter (4.08%)	_model (3.69%)	_test (3.40%)	_which (3.11%)	_neural (3.55%)	verse (3.82%)	_Cube (3.66%)
Block 10 (10.50%)	. (16.50%)	lists (9.61%)	g (4.99%)	_of (16.60%)	_which (11.47%)	_neural (5.79%)	_neural (3.50%)	_is (15.56%)
Block 11 (25.30%)	, (16.96%)	" (27.59%)	_networks (28.89%)	" (24.52%)	_the (26.92%)	_new (29.14%)	m (22.95%)	_neural (25.40%)
Block 12 (25.13%)	, (6.56%)	. (28.62%)	net (29.35%)	, (26.40%)	the (27.77%)	the (29.85%)	c (25.27%)	. (27.23%)
Logits	,	-	_network	_that	_which	_neural	ient	_is
Expan. (1.000)	,	-	_network	_of	_which	"	-	_is

Figure 13: Joint jet lens with learnable weightings ($k = 0$), applied over GPT2 with the input sentence "new simple neural architecture, the Transformer"

	new	_simple	_neural	_architecture	,	_the	_Trans	former
Block 1 (15.30%)	. (7.49%)	" (16.78%)	_networks (16.96%)	", (18.37%)	_neural (14.61%)	_neural (14.05%)	verse (16.45%)	_Neural (17.73%)
Block 2 (4.57%)	, (13.81%)	json (3.21%)	_networks (3.29%)	_model (3.46%)	_which (3.11%)	_neural (3.02%)	cend (3.23%)	_Neural (3.45%)
Block 3 (4.49%)	, (14.25%)	tons (3.25%)	_networks (2.82%)	_architecture (3.32%)	_neural (3.10%)	_neural (3.00%)	porter (3.03%)	_Neural (3.17%)
Block 4 (4.10%)	. (11.55%)	tons (3.28%)	_networks (3.27%)	_leveraging (3.19%)	_synt (3.04%)	_neural (2.98%)	verse (2.90%)	_Neural (2.57%)
Block 5 (4.02%)	. (9.58%)	tons (3.05%)	_networks (3.25%)	_algorithm (3.45%)	_which (3.14%)	_neural (2.99%)	mitter (3.24%)	_Neural (3.47%)
Block 6 (3.02%)	. (2.75%)	_linkage (2.65%)	_net (3.04%)	_algorithms (3.26%)	_detecting (2.94%)	_neural (2.80%)	cend (3.30%)	_Neural (3.45%)
Block 7 (2.91%)	. (2.98%)	_teleportation (2.78%)	_nets (3.19%)	_approach (3.24%)	_specifically (2.49%)	_cortex (2.58%)	genic (3.07%)	_Cortex (2.95%)
Block 8 (4.60%)	bid (3.10%)	nex (7.64%)	_network (2.63%)	_platform (2.62%)	_neural (4.81%)	_participant (9.06%)	cription (3.50%)	_Neural (3.45%)
Block 9 (7.44%)	iaries (3.10%)	url (5.60%)	_networks (7.77%)	_intelligence (4.86%)	_Torch (14.64%)	_welcoming (13.48%)	Secure (7.21%)	_conv (2.83%)
Block 10 (15.04%)	akings (13.99%)	widget (14.80%)	_network (16.20%)	_None (13.05%)	_Bund (15.37%)	_safest (14.72%)	cend (16.11%)	_disabling (16.06%)
Block 11 (16.50%)	ity (3.19%)	ton (18.47%)	_network (18.79%)	_architecture (20.49%)	_which (16.34%)	_neural (15.62%)	istor (18.84%)	ãĦ¢ (20.28%)
Block 12 (18.00%)	, (14.21%)	- (18.49%)	network (18.78%)	that (20.68%)	which (16.41%)	neural (15.70%)	ient (19.11%)	is (20.60%)
Logits	,	-	_network	_that	_which	_neural	ient	_is
Expan. (1.000)	akings	json	_networks	_framework	_neural	_neural	cend	_Neural

Figure 14: Joint jet lens with learnable weightings ($k = 1$), applied over GPT2 with the input sentence "new simple neural architecture, the Transformer"

	new	_simple	_neural	_architecture	,	_the	_Trans	former
Block 1 (3.58%)	Supporters (1.55%)	Supporters (3.24%)	Supporters (3.46%)	Supporters (5.37%)	Supporters (5.08%)	Supporters (3.52%)	Supporters (3.88%)	Supporters (2.56%)
Block 2 (2.13%)	foreseen (1.61%)	foreseen (2.97%)	foreseen (1.15%)	Introduced (3.96%)	foreseen (1.09%)	foreseen (1.54%)	Supporters (3.67%)	Supporters (1.03%)
Block 3 (2.07%)	Amid (1.65%)	Supporters (2.01%)	Across (1.32%)	gewater (1.14%)	Supporters (3.66%)	Supporters (2.93%)	Supporters (2.58%)	leground (1.28%)
Block 4 (1.57%)	_impover (1.97%)	_unpop (2.18%)	_unpop (1.46%)	_impover (1.33%)	_impover (1.39%)	_impover (1.71%)	_uphe (1.27%)	_impover (1.27%)
Block 5 (1.47%)	Attempts (1.76%)	_municip (2.15%)	_airst (1.45%)	_linem (1.29%)	amiliar (1.32%)	pelling (1.38%)	rieving (1.26%)	_linem (1.13%)
Block 6 (1.45%)	Residents (1.76%)	_athlet (2.17%)	rha (1.44%)	_twent (1.34%)	_way (1.05%)	ters (1.40%)	rha (1.23%)	_Xuan (1.25%)
Block 7 (3.57%)	Ironically (1.63%)	celona (2.74%)	wrap (3.78%)	_look (5.71%)	_airstrike (1.22%)	_equivalent (2.63%)	_different (6.30%)	_hollow (4.58%)
Block 8 (4.63%)	Supporters (1.61%)	imura (3.91%)	vantage (3.03%)	anoia (5.48%)	foreseen (6.13%)	ileen (4.55%)	Enlarge (5.70%)	assador (6.59%)
Block 9 (3.14%)	Ironically (1.65%)	erguson (2.00%)	certain (2.53%)	OUR (1.28%)	_local (3.54%)	erguson (1.80%)	enter (5.43%)	bec (6.89%)
Block 10 (1.73%)	foreseen (1.65%)	foreseen (2.01%)	Engineers (1.20%)	Engineers (2.88%)	asury (1.19%)	thinkable (1.40%)	Attempts (2.53%)	uddenly (0.96%)
Block 11 (1.71%)	likely (1.57%)	extremely (1.88%)	aples (1.18%)	_screenplay (1.29%)	earances (1.30%)	earances (4.13%)	oother (1.20%)	_resurg (1.12%)
Block 12 (4.53%)	Ironically (1.73%)	Phones (3.91%)	ADVERTISEMENT (4.39%)	ADVERTISEMENT (6.03%)	isively (4.65%)	_Blvd (4.46%)	ADVERTISEMENT (6.08%)	ADVERTISEMENT (4.99%)
Block 13 (2.80%)	_a (1.68%)	aji (2.83%)	imbabwe (1.33%)	rone (1.28%)	OTOS (5.38%)	ppard (3.08%)	ppard (1.07%)	aji (5.76%)
Block 14 (2.91%)	foreseen (1.66%)	ADVERTISEMENT (1.83%)	Marginal (3.82%)	chell (1.32%)	_Appalach (1.33%)	_Caucasus (4.66%)	_still (5.47%)	, (3.23%)
Block 15 (1.47%)	ormons (1.78%)	_confir (1.89%)	uring (1.34%)	ured (1.25%)	_AoE (1.38%)	_Caucas (1.68%)	_lineman (1.25%)	_topple (1.22%)
Block 16 (3.98%)	Against (1.82%)	folios (1.93%)	@ (6.49%)	thinkable (3.49%)	_tsun (1.26%)	_D (4.65%)	I (5.84%)	arsh (6.38%)
Block 17 (2.89%)	urses (1.38%)	untled (4.46%)	ortunate (3.72%)	ithub (1.21%)	_our (4.69%)	ortment (1.51%)	erenn (4.91%)	ombies (1.21%)
Block 18 (5.12%)	foreseen (1.63%)	Supporters (4.53%)	Nonetheless (6.62%)	Ironically (5.07%)	Thankfully (5.66%)	Shortly (4.52%)	af (5.80%)	_js (7.12%)
Block 19 (2.96%)	pherd (1.47%)	_enough (4.91%)	ag (3.58%)	_for (5.69%)	incerity (1.08%)	incerity (2.75%)	extreme (3.01%)	phabet (1.21%)
Block 20 (5.68%)	Ċ (2.06%)	Ċ (5.07%)	_just (7.05%)	Ċ (6.91%)	Attempts (6.51%)	paralleled (4.49%)	- (6.53%)	, (6.87%)
Block 21 (1.46%)	ription (1.60%)	ription (2.15%)	_Playoffs (1.48%)	isdom (1.06%)	_frontrunner (1.36%)	_frontrunner (1.69%)	_TBD (1.24%)	pered (1.06%)
Block 22 (4.55%)	_in (3.36%)	_first (5.29%)	_two (7.06%)	_one (6.98%)	_which (6.97%)	_one (4.56%)	_isEnabled (1.03%)	elligence (1.15%)
Block 23 (5.21%)	, (4.80%)	)) (5.23%)	_* (7.13%)	) (6.26%)	_while (6.31%)	_point (4.57%)	albeit (1.15%)	B (6.21%)
Block 24 (6.13%)	_a (5.62%)	_m (5.26%)	_first (7.18%)	_for (7.33%)	_the (7.33%)	_so (4.70%)	_trans (5.70%)	rieving (5.90%)
Block 25 (1.55%)	foreseen (1.67%)	acly (2.14%)	_enthus (1.49%)	_anecd (1.35%)	_trainers (1.43%)	_subreddits (1.74%)	ithub (1.28%)	_Trainer (1.27%)
Block 26 (2.61%)	- (6.25%)	_simple (2.08%)	_simple (5.95%)	ername (1.30%)	haar (1.34%)	_satell (1.74%)	igsaw (1.02%)	_headphone (1.17%)
Block 27 (2.65%)	_âĢ (7.40%)	_âĢ (5.48%)	_OSM (1.35%)	held (1.30%)	dayName (1.38%)	_artif (1.75%)	--+ (1.27%)	_nostalg (1.30%)
Block 28 (2.39%)	_fps (8.56%)	>>\ (2.30%)	_Oo (1.42%)	_tacos (1.30%)	_msec (1.41%)	_unbeliev (1.75%)	_hrs (1.12%)	_reminis (1.28%)
Block 29 (1.97%)	_âĢ¦ (5.17%)	_convol (2.18%)	ricanes (1.47%)	_Gujar (1.25%)	acerb (1.38%)	cffff (1.74%)	_negoti (1.28%)	_automakers (1.27%)
Block 30 (1.84%)	_âĢ¦ (4.01%)	_anecd (2.24%)	_unve (1.49%)	_overwhel (1.37%)	!?* (1.43%)	20439 (1.78%)	_negoti (1.29%)	_calculates (1.12%)
Block 31 (4.61%)	!!* (8.40%)	_âĢ¦ (2.57%)	_greets (1.35%)	_entert (1.80%)	\\\\ (4.44%)	\\\\ (6.14%)	*! (5.27%)	?/ (6.88%)
Block 32 (5.64%)	âĢ¦" (9.55%)	!?* (4.42%)	âĢ¦" (2.29%)	âĢ¦" (5.37%)	_âĢ¦" (6.35%)	_\' (9.03%)	©¶æ¥µ (3.34%)	âĢ¦" (4.75%)
Logits	_	_	_network	_for	_which	_neural	former	,
Expan. (0.977)	_the	_and	-	_for	_the	_first	-	,

Figure 15: Joint jet lens with learnable weightings ($k = 0$), applied over GPT-Neo-2.7B with the input sentence "new simple neural architecture, the Transformer"

	new	_simple	_neural	_architecture	,	_the	_Trans	former
Block 1 (7.36%)	, (3.40%)	ton (8.06%)	_network (8.57%)	_for (8.22%)	_which (7.51%)	_first (7.30%)	former (7.43%)	, (8.36%)
Block 2 (4.83%)	- (2.39%)	_ (5.23%)	_network (6.91%)	_for (4.98%)	_which (4.60%)	_neural (4.77%)	former (5.09%)	, (4.68%)
Block 3 (1.31%)	_File (1.62%)	_ (1.29%)	_network (1.31%)	_for (1.28%)	_which (1.25%)	_CNN (1.22%)	former (1.20%)	, (1.32%)
Block 4 (7.81%)	_impover (5.74%)	_unpop (8.48%)	_impover (8.76%)	_impover (8.45%)	_impover (7.67%)	_Neural (7.51%)	former (7.39%)	_Networks (8.45%)
Block 5 (1.79%)	User (5.29%)	_ (1.31%)	_network (1.30%)	_for (1.29%)	_which (1.29%)	_neural (1.26%)	former (1.25%)	, (1.31%)
Block 6 (1.79%)	Instance (5.33%)	_ (1.33%)	_network (1.31%)	_for (1.29%)	_which (1.26%)	_neural (1.23%)	former (1.23%)	, (1.32%)
Block 7 (1.59%)	File (3.56%)	_ (1.37%)	_network (1.36%)	_for (1.33%)	_which (1.28%)	_neural (1.24%)	former (1.25%)	, (1.32%)
Block 8 (1.70%)	Supporters (5.02%)	_ (1.29%)	_network (1.28%)	_for (1.25%)	_which (1.24%)	_Neural (1.17%)	former (1.12%)	, (1.21%)
Block 9 (1.77%)	Enlarge (5.04%)	_ (1.37%)	_network (1.37%)	_for (1.32%)	_which (1.26%)	_neural (1.23%)	former (1.25%)	, (1.31%)
Block 10 (4.41%)	foreseen (5.36%)	_ (5.77%)	_network (6.19%)	_for (5.99%)	_which (1.15%)	_neural (0.93%)	former (2.45%)	, (7.42%)
Block 11 (1.31%)	, (1.90%)	_ (1.30%)	_network (1.29%)	_for (1.20%)	_which (1.18%)	_neural (1.19%)	former (1.19%)	, (1.24%)
Block 12 (1.21%)	, (1.74%)	_ (1.11%)	_network (1.17%)	_for (1.10%)	_which (1.16%)	_neural (1.15%)	former (1.07%)	, (1.21%)
Block 13 (1.37%)	_ (1.94%)	_ (1.36%)	_network (1.35%)	_for (1.32%)	_which (1.23%)	_neural (1.21%)	former (1.23%)	, (1.32%)
Block 14 (1.22%)	, (1.82%)	_ (1.18%)	_network (1.22%)	_for (1.12%)	_which (1.15%)	_neural (1.09%)	former (1.04%)	, (1.12%)
Block 15 (1.34%)	_ (1.90%)	_ (1.33%)	_network (1.31%)	_for (1.29%)	_which (1.21%)	_neural (1.20%)	former (1.20%)	, (1.28%)
Block 16 (1.31%)	((1.91%)	_ (1.28%)	_network (1.28%)	_for (1.24%)	_which (1.18%)	_neural (1.19%)	former (1.18%)	_model (1.23%)
Block 17 (1.31%)	_ (1.90%)	_ (1.29%)	_network (1.28%)	_for (1.26%)	_which (1.14%)	_neural (1.12%)	former (1.16%)	, (1.29%)
Block 18 (4.55%)	, (1.65%)	_ (5.16%)	_network (3.55%)	_for (5.49%)	_which (6.28%)	_neural (6.05%)	former (5.05%)	, (3.17%)
Block 19 (1.24%)	, (1.84%)	_ (1.23%)	_network (1.17%)	_for (1.18%)	_which (1.23%)	_neural (0.97%)	former (1.10%)	_model (1.18%)
Block 20 (3.30%)	Ċ (1.84%)	_ (2.30%)	_network (1.16%)	_for (4.21%)	_which (6.29%)	_neural (5.89%)	former (2.70%)	_architecture (2.00%)
Block 21 (1.87%)	_ (1.80%)	_ (1.21%)	_network (1.12%)	_for (1.15%)	_which (3.82%)	_neural (3.71%)	former (1.10%)	, (1.02%)
Block 22 (4.81%)	- (1.91%)	_infographic (8.14%)	_network (3.50%)	_outper (5.92%)	_which (6.89%)	_neural (6.76%)	former (1.57%)	_[(3.83%)
Block 23 (2.01%)	, (1.91%)	_ (1.14%)	_network (1.40%)	_learns (1.38%)	_which (3.94%)	_Conv (3.99%)	former (1.14%)	_model (1.18%)
Block 24 (6.02%)	, (1.94%)	_infographic (8.04%)	_network (7.20%)	_unve (8.00%)	_unve (7.47%)	_Neural (7.02%)	former (3.53%)	_model (4.98%)
Block 25 (1.19%)	_ (1.87%)	_ (1.19%)	_network (1.09%)	_for (1.22%)	_which (0.96%)	_âĢ (1.07%)	former (1.06%)	, (1.04%)
Block 26 (1.55%)	_ (1.89%)	_ (1.18%)	_network (2.18%)	_called (1.22%)	_which (1.25%)	_Conv (1.09%)	former (2.57%)	, (1.06%)
Block 27 (2.23%)	_ (1.93%)	ton (3.53%)	_network (1.09%)	_for (1.21%)	_which (0.99%)	_model (1.13%)	former (6.67%)	, (1.25%)
Block 28 (2.76%)	_ (1.73%)	json (1.02%)	_network (3.49%)	_for (1.84%)	_which (0.95%)	_Neural (3.31%)	former (6.31%)	, (3.42%)
Block 29 (3.22%)	_âĢ¦" (6.01%)	_ (1.32%)	_network (1.00%)	_for (1.01%)	_and (1.74%)	_neural (1.90%)	former (7.25%)	, (5.54%)
Block 30 (6.24%)	_âĢ¦" (6.04%)	_ (3.56%)	_network (7.34%)	_for (5.45%)	_which (6.05%)	_neural (6.14%)	former (7.30%)	Âł (8.04%)
Block 31 (7.76%)	!!" (5.96%)	(8.27%)	_network (8.68%)	_for (8.36%)	_the (7.67%)	_Conv (7.46%)	former (7.35%)	, (8.37%)
Block 32 (7.84%)	âĢ¦." (5.81%)	!?" (8.35%)	_network (8.78%)	, (8.43%)	_and (7.70%)	_neural (7.51%)	former (7.57%)	_model (8.53%)
Logits	_	_	_network	_for	_which	_neural	former	,
Expan. (0.993)	_	_	_network	_for	_which	_neural	former	,

Figure 16: Joint jet lens with learnable weightings ($k = 1$), applied over GPT-Neo-2.7B with the input sentence "new simple neural architecture, the Transformer"

	new	_simple	_neural	_architecture	,	_the	_Trans	former
Block 1 (3.19%)	bie (4.48%)	_simple (4.99%)	_neural (0.98%)	_architecture (1.08%)	_and (5.08%)	_the (5.85%)	fig (2.07%)	former (1.01%)
Block 2 (1.81%)	_arrivals (2.43%)	tons (1.22%)	_rack (3.83%)	_model (1.07%)	_the (1.01%)	_main (1.01%)	ient (3.10%)	_generation (0.85%)
Block 3 (2.49%)	_entry (5.53%)	_fitting (5.41%)	_clusters (3.05%)	_det (1.14%)	_thanks (0.99%)	_second (1.00%)	cription (0.97%)	_barrier (1.86%)
Block 4 (3.02%)	bies (3.47%)	_private (5.64%)	_env (5.41%)	_clusters (1.18%)	_aspirin (1.09%)	_hypothesis (1.08%)	cript (5.55%)	_Mund (0.75%)
Block 5 (1.75%)	_mansion (3.47%)	_Transcript (1.03%)	ous (2.48%)	_suit (1.15%)	chuk (1.11%)	_Oracle (1.17%)	_Card (2.55%)	cknow (1.00%)
Block 6 (1.84%)	_Parables (2.46%)	_Bald (1.45%)	izer (0.99%)	sche (1.21%)	%); (1.11%)	lija (1.18%)	ione (5.34%)	atti (1.01%)
Block 7 (2.51%)	DERR (2.47%)	_sp (1.62%)	_wired (3.21%)	inea (1.19%)	)* (1.02%)	_gloss (1.17%)	aways (4.96%)	_system (4.48%)
Block 8 (1.80%)	, (2.32%)	_Tall (1.04%)	_experiments (0.89%)	MIT (1.21%)	mac (1.06%)	fts (1.16%)	rock (5.75%)	con (0.97%)
Block 9 (1.79%)	, (2.19%)	onel (1.11%)	_layer (5.70%)	_hum (1.10%)	arily (1.06%)	_Hots (1.20%)	iter (0.98%)	_boxes (0.96%)
Block 10 (2.17%)	, (2.18%)	tested (1.09%)	/ (6.21%)	_deployed (1.18%)	_disrupt (3.01%)	ew (1.11%)	_INS (0.76%)	_Drive (1.80%)
Block 11 (1.20%)	, (2.18%)	azon (1.10%)	âĥ¹âĤ (1.00%)	ea (1.20%)	Ro (1.10%)	_Dive (1.10%)	_Revised (0.95%)	_Prol (1.00%)
Block 12 (1.17%)	, (2.20%)	_Think (1.05%)	_Dish (0.86%)	_Layer (1.11%)	_Sing (0.99%)	uts (1.16%)	_button (0.94%)	_proble (1.02%)
Block 13 (1.88%)	_and (2.22%)	_ab (2.77%)	ourt (4.71%)	_Malf (1.20%)	_REPL (0.99%)	_naked (1.17%)	oran (0.98%)	_cred (1.01%)
Block 14 (1.60%)	_and (2.22%)	alg (1.06%)	_underestimated (0.97%)	_percentile (1.19%)	_which (2.35%)	_nonetheless (1.15%)	igo (3.05%)	_Hut (0.81%)
Block 15 (2.19%)	_and (2.24%)	- (4.45%)	_Subst (1.01%)	chan (1.16%)	ATURES (1.09%)	_hitch (1.19%)	_Mini (0.99%)	_Bre (5.41%)
Block 16 (2.24%)	_and (2.26%)	_image (5.83%)	_cell (4.89%)	_packs (1.05%)	_marked (0.91%)	_Finn (1.09%)	omes (0.89%)	_Cipher (0.99%)
Block 17 (1.72%)	_and (2.27%)	Âŀ (1.11%)	_formulation (0.96%)	isen (1.22%)	_modular (1.08%)	_Space (0.99%)	_Neural (0.85%)	_Trainer (5.29%)
Block 18 (1.54%)	_and (2.21%)	_bond (1.06%)	_IPM (1.01%)	_[(4.36%)	build (0.97%)	plex (1.04%)	brand (0.78%)	_Quest (0.91%)
Block 19 (2.17%)	_and (2.13%)	_cross (3.75%)	_proceeds (5.61%)	_named (2.11%)	_called (0.93%)	_parallel (1.08%)	Shares (0.96%)	_lost (0.81%)
Block 20 (2.64%)	, (3.62%)	": (0.98%)	rons (1.15%)	_Neural (2.26%)	_coupled (4.39%)	_omn (2.30%)	fect (4.73%)	_Fly (1.73%)
Block 21 (1.27%)	, (3.47%)	_ft (0.97%)	ysis (1.03%)	_template (1.09%)	_with (0.83%)	_latter (1.09%)	adic (0.79%)	âĦ¢ (0.87%)
Block 22 (3.88%)	, (3.56%)	types (0.98%)	_Turing (2.15%)	. (7.00%)	_which (4.55%)	_most (5.96%)	gress (1.06%)	_VT (5.74%)
Block 23 (3.17%)	, (3.95%)	tv (1.07%)	blade (0.96%)	_.* (1.16%)	_i (2.87%)	_model (5.98%)	du (4.83%)	_erg (4.52%)
Block 24 (5.36%)	, (3.89%)	_prayers (5.37%)	_Turing (6.05%)	, (6.95%)	_which (5.59%)	_brain (6.37%)	Memory (5.62%)	als (3.00%)
Block 25 (2.84%)	, (3.80%)	_complex (0.86%)	_surgery (0.93%)	* (0.97%)	_Neural (1.57%)	_one (5.52%)	_EEG (3.47%)	, (5.60%)
Block 26 (5.61%)	, (3.63%)	_dot (6.73%)	_Turing (6.16%)	_for (7.62%)	_then (6.26%)	_Neural (5.36%)	ocy (5.16%)	_robot (3.94%)
Block 27 (4.91%)	, (3.64%)	?" (7.12%)	_algorithm (2.21%)	", (6.61%)	_where (5.86%)	_so (5.87%)	vier (1.80%)	_or (6.21%)
Block 28 (3.91%)	, (2.94%)	_solution (0.91%)	_simulation (4.19%)	", (5.57%)	_which (5.97%)	_F (6.14%)	inil (0.95%)	_Mega (4.63%)
Block 29 (4.07%)	, (1.51%)	_life (6.69%)	_network (2.58%)	) (2.36%)	_using (5.32%)	_neural (6.09%)	Washington (4.30%)	_brains (3.73%)
Block 30 (5.05%)	, (1.96%)	ÃĿ (5.52%)	_net (5.50%)	_that (7.83%)	_neural (6.24%)	_neural (6.05%)	_underground (4.91%)	_Brain (2.39%)
Block 31 (5.02%)	, (2.04%)	" (6.84%)	_Machine (3.46%)	," (7.99%)	_neural (6.56%)	_neural (6.10%)	onet (0.95%)	_neural (6.19%)
Block 32 (5.00%)	, (2.06%)	' (5.21%)	_net (0.94%)	' (7.68%)	_called (6.27%)	_simple (6.34%)	haus (5.11%)	3 (6.41%)
Block 33 (3.65%)	, (2.08%)	'' (0.83%)	_assembly (5.90%)	' (1.61%)	_to (5.86%)	_TW (1.51%)	Global (5.96%)	_LL (5.41%)
Block 34 (2.57%)	, (2.10%)	_to (1.01%)	_vide (0.99%)	. (2.72%)	_and (1.15%)	_class (1.00%)	lc (5.89%)	, (5.73%)
Block 35 (1.67%)	, (2.12%)	client (1.09%)	_NET (1.00%)	Ċ (3.33%)	_and (2.74%)	_reservoir (1.16%)	Draft (1.02%)	_scripts (0.93%)
Block 36 (1.28%)	ċ (2.69%)	Ċ (1.06%)	gil (1.03%)	Ċ (1.15%)	Ċ (1.01%)	_Leopard (1.22%)	artist (1.05%)	stals (1.02%)
Logits	_	"	_network	'	_which	_neural	ċ	,
Expan. (0.980)	,	-	_network	_for	_which	_neural	-	,

Figure 17: Joint jet lens with learnable weightings ($k = 0$), applied over GPT-2-large with the input sentence "new simple neural architecture, the Transformer"

	new	_simple	_neural	_architecture	,	_the	_Trans	former
Block 1 (3.50%)	bie (3.17%)	" (4.75%)	_network (5.93%)	" (3.61%)	_which (1.15%)	_neural (1.60%)	c (5.06%)	_is (2.74%)
Block 2 (3.14%)	_ (0.84%)	" (4.15%)	_network (5.49%)	' (1.80%)	_which (4.28%)	_neural (4.04%)	c (3.60%)	_is (0.93%)
Block 3 (1.19%)	_ (0.86%)	" (0.91%)	_network (0.84%)	' (1.05%)	_which (1.81%)	_neural (2.17%)	c (0.78%)	_is (1.08%)
Block 4 (1.08%)	- (0.77%)	ton (1.88%)	_network (1.27%)	' (0.99%)	_we (0.96%)	_neural (0.94%)	c (0.75%)	_is (1.07%)
Block 5 (0.98%)	_ (0.74%)	" (1.03%)	_network (0.98%)	' (1.06%)	_where (1.01%)	_brain (1.00%)	c (0.88%)	_is (1.13%)
Block 6 (1.29%)	_ (3.29%)	" (1.01%)	_network (0.93%)	' (1.07%)	_and (1.00%)	_neural (1.00%)	c (0.93%)	_is (1.06%)
Block 7 (1.32%)	_ (3.60%)	" (1.04%)	_network (0.97%)	' (1.10%)	_which (1.00%)	_neural (1.00%)	parent (0.89%)	_is (0.97%)
Block 8 (1.35%)	_ (3.71%)	" (1.05%)	_network (0.95%)	' (1.07%)	_which (0.98%)	_researchers (0.99%)	ient (0.97%)	_is (1.10%)
Block 9 (1.44%)	, (3.74%)	" (1.04%)	_network (0.83%)	' (1.07%)	_which (0.99%)	_neural (0.99%)	c (0.94%)	_is (1.91%)
Block 10 (1.47%)	- (3.73%)	" (1.04%)	_network (1.44%)	' (1.07%)	_which (0.97%)	_neural (0.99%)	former (0.93%)	_AI (1.57%)
Block 11 (1.36%)	- (3.71%)	" (0.98%)	_network (1.01%)	' (1.12%)	_which (0.98%)	_neural (0.98%)	c (0.99%)	_is (1.10%)
Block 12 (1.36%)	_ (3.69%)	" (1.00%)	_network (1.04%)	' (1.08%)	_which (0.97%)	_neural (0.97%)	c (1.03%)	, (1.12%)
Block 13 (1.35%)	_ (3.65%)	" (1.01%)	_network (1.04%)	" (1.10%)	_where (0.96%)	_neural (0.96%)	c (1.01%)	_Cortex (1.09%)
Block 14 (1.31%)	_ (3.61%)	" (1.00%)	_network (1.02%)	' (1.07%)	_a (0.74%)	_neural (0.92%)	ient (1.00%)	_is (1.10%)
Block 15 (1.30%)	_ (3.54%)	" (0.99%)	_network (1.03%)	' (1.07%)	_which (0.93%)	_neural (0.93%)	c (1.00%)	_chip (0.90%)
Block 16 (1.30%)	_ (3.43%)	" (1.04%)	_network (0.95%)	' (1.09%)	_and (0.89%)	_neural (0.89%)	c (0.99%)	, (1.13%)
Block 17 (1.28%)	_ (3.36%)	" (0.97%)	_network (0.95%)	' (1.09%)	_which (0.90%)	_neural (0.86%)	c (0.99%)	. (1.10%)
Block 18 (1.14%)	_ (2.81%)	_ (0.92%)	_network (1.00%)	' (0.90%)	_a (0.74%)	_more (0.79%)	c (0.90%)	_chip (1.09%)
Block 19 (0.99%)	_ (0.98%)	" (0.84%)	_network (0.88%)	' (0.95%)	_or (1.44%)	_neural (0.76%)	c (0.98%)	_architecture (1.10%)
Block 20 (1.53%)	, (0.95%)	x (0.88%)	_network (0.95%)	' (0.99%)	_we (3.52%)	_authors (3.11%)	c (0.77%)	_is (1.07%)
Block 21 (1.23%)	, (0.96%)	" (0.86%)	_networks (0.90%)	' (1.04%)	_neural (1.93%)	_network (1.16%)	c (1.93%)	_is (1.07%)
Block 22 (1.92%)	- (0.96%)	" (2.47%)	_network (0.88%)	' (1.05%)	_we (4.10%)	_neural (4.13%)	c (0.78%)	_Brain (0.98%)
Block 23 (2.10%)	_ (0.90%)	_stuff (0.79%)	_network (1.16%)	' (0.85%)	_similar (3.67%)	_cu (4.65%)	c (3.79%)	_is (0.99%)
Block 24 (3.00%)	_ (0.93%)	" (2.25%)	_network (4.69%)	' (2.88%)	' (4.60%)	_ART (4.85%)	c (2.96%)	, (0.85%)
Block 25 (3.99%)	"]=> (3.39%)	ton (4.25%)	_net (2.85%)	' (2.19%)	_with (4.38%)	_loc (4.88%)	c (5.43%)	_5 (4.59%)
Block 26 (3.96%)	Instance (3.52%)	' (3.67%)	_network (3.98%)	' (4.45%)	_Cooper (4.93%)	_first (4.80%)	c (4.25%)	, (2.07%)
Block 27 (4.99%)	_ (3.24%)	tons (5.87%)	_network (4.56%)	_of (5.90%)	_but (4.78%)	_neuron (4.83%)	c (4.85%)	_Memory (5.85%)
Block 28 (5.13%)	_ (3.08%)	ton (5.20%)	_network (5.48%)	_for (5.93%)	_NI (4.98%)	_first (4.92%)	ient (5.17%)	_uses (6.28%)
Block 29 (5.04%)	_ (3.27%)	me (5.80%)	_network (5.64%)	". (5.22%)	_NAT (4.95%)	_authors (4.94%)	ient (5.52%)	_3000 (5.00%)
Block 30 (4.88%)	_ (3.40%)	_kitchen (4.88%)	_network (5.69%)	" (5.41%)	_prototyp (4.94%)	_algorithm (4.88%)	ient (5.55%)	_uses (4.30%)
Block 31 (5.31%)	_ (3.61%)	x (6.06%)	_network (3.85%)	' (6.79%)	_geared (5.16%)	_traditional (5.00%)	c (5.28%)	_XL (6.76%)
Block 32 (5.51%)	- (3.70%)	_white (5.66%)	_network (5.56%)	" (6.48%)	", (5.09%)	_WS (5.03%)	c (5.33%)	_is (7.26%)
Block 33 (5.75%)	, (3.73%)	" (6.05%)	_network (6.01%)	" (6.91%)	_which (5.15%)	_neural (5.05%)	c (5.66%)	_Robot (7.46%)
Block 34 (5.88%)	, (3.73%)	ton (6.26%)	_network (6.49%)	", (6.91%)	_which (5.15%)	_neural (5.04%)	ient (5.96%)	_Cortex (7.50%)
Block 35 (5.77%)	- (3.74%)	" (6.11%)	_network (6.26%)	_model (6.90%)	_modeled (5.03%)	_neural (4.97%)	ient (6.03%)	_model (7.17%)
Block 36 (5.85%)	_ (3.67%)	" (6.29%)	_network (6.51%)	' (6.77%)	_which (4.95%)	_neural (5.00%)	c (6.10%)	_is (7.52%)

Logits	_	"	_network	'	_which	_neural	c	_is
Expan. (0.994)	_	"	_network	'	_and	_neural	c	_is

Figure 18: Joint jet lens with learnable weightings ($k = 1$), applied over GPT-2-large with the input sentence "new simple neural architecture, the Transformer"